AD NUMBER
AD812801
NEW LIMITATION CHANGE
TO Approved for public release, distribution unlimited
FROM Distribution authorized to U.S. Gov't. agencies and their contractors; Critical Technology; DEC 1966. Other requests shall be referred to Air Force Materials Laboratory, Attn: Research and Technology Div. [MAAE], Wright-Patterson AFB, OH 45433.
AUTHORITY
AFML ltr dtd 12 Jan 1972

AFML-TR-66-232

EFFECT OF SURFACE ROUGHNESS ON THE REFLECTANCE OF REFRACTORY METALS

DONALD F. STEVISON

TECHNICAL REPORT AFML-TR-66-232

DECEMBER 1966

AIR FORCE MATERIALS LABORATORY
RESEARCH AND TECHNOLOGY DIVISION
AIR FORCE SYSTEMS COMMAND
WRIGHT-PATTERSON AIR FORCE BASE, OHIO

NOTICES

When Government drawings, specifications, or other data are used for any purpose other than in connection with a definitely related Government procurement operation, the United States Government thereby incurs no responsibility nor any obligation whatsoever; and the fact that the Government may have formulated, furnished, or in any way supplied the said drawings, specifications, or other data, is not to be regarded by implication or otherwise as in any manner licensing the holder or any other person or corporation, or conveying any rights or permission to manufacture, use, or sell any patented invention that may in any way be related thereto.

Copies of this report should not be returned to the Research and Technology Division unless return is required by security considerations, contractual obligations, or notice on a specific document.

AFML-TR-66-232

EFFECT OF SURFACE ROUGHNESS ON THE REFLECTANCE OF REFRACTORY METALS

DONALD F. STEVISON

FOREWORD

This report was prepared by the Materials Engineering Branch, Materials Applications Division, Air Force Materials Laboratory. The work was conducted under Project No. 7381, "Materials Applications," Task No. 738102, "Materials Processes," and was administered by the Air Force Materials Laboratory, Research and Technology Division, Air Force Systems Command, Wright-Patterson Air Force Base, Ohio, Donald F. Stevison, Project Engineer. The effort was funded in part by the Director's Fund.

This report covers work carried out during the period 1 May 1965 to 1 May 1966. The manuscript was released by the author in June 1966 for publication as a technical report.

The author is indebted to G. V. Purcell, 1/Lt, USAF, for valuable discussions concerning this investigaion and for reviewing the manuscript.

This technical report has been reviewed and is approved.

A. OLEVITCH
Chief, Materials Engineering Branch
Materials Applications Division
Air Force Materials Laboratory

ABSTRACT

The influence of surface roughness on the thermal optical properties (reflectance and emittance) of three refractory materials, columbium alloy, D-36, tantalum and tungsten has been studied. Current data obtained by different investigators for the same materials have varied more than 50 percent. Several investigators studying the interaction of radiation with rough surfaces have developed theoretical approaches to correlate thermal optical properties with the material being studied; however, no predictions have been made as to the magnitude of the surface effects. This report establishes several general trends in this direction.

A Perkin-Elmer model 13U Spectrophotometer with a model 205 Reflectance-Emittance attachment was used for all reflectance an emittance measurements. A Taylor-Hobson Talysurf was used to measure the surface roughness of each sample. Two surface roughness preparations were used - random sanding and sandblasting.

As a typical example of the results, the total hemispherical reflectance of tantalum was changed 26 percent at short wavelengths and 25 percent at longer wavelengths by surface roughness values ranging from 0.192 to 3.0 AA microns. The specular reflectance of tantalum changed 56 percent at short wavelengths and 75 percent at long wavelengths for the same range of surface roughness values. Material effects caused a maximum difference of only 16 percent in the total hemispherical reflectance of these three refractory materials; however, the maximum change in surface roughness caused the total hemispherical reflectance to vary 20 to 40 percent as a function of wavelength.

The influence of second order effects has been observed. The degree to which emittance influences the surface temperature and incident heat flux capabilities of materials is discussed.

TABLE OF CONTENTS

TABLE OF CONTENTS (cont'd)

ILLUSTRATIONS

ILLUSTRATIONS (Cont'd)

ILLUSTRATIONS (Cont'd)

TABLES

SECTION I

INTRODUCTION

1. OBJECTIVE

The objective of this study was to investigate the effect of surface roughness on the thermal optical properties (emittance and reflectance) of metals. These properties are important to the design and performance of future space systems since the radiant heat transfer characteristics of these systems will depend to a great extent on the optical characteristics of their surfaces. The overall system temperature may often be established by surface emittance and reflectance values. As a further example, space radiator size and weight is generally inversely related to surface emittance. From a heat transfer standpoint, analysis of the temperature of a surface or structure as a whole is complicated by other nearby surfaces and structures because the direction-intensity parameters of the reflected solar flux are not known.

2. BACKGROUND

In many cases reported thermal optical property data are contradictory or are entirely unavailable. Current data obtained by different investigators on the same material have varied more than 50 percent in some instances (Reference 1). The differences are due to poor experimental techniques, improper preparation of samples, inadequate definition of experimental conditions, or poor instrumentation. In many cases the data from different investigators cannot be satisfactorily compared or correlated due to insufficient information concerning the physical, chemical, and geometrical nature of the test specimen surfaces. Thus, increased attention must be given to the fundamental factors affecting the thermal radiation characteristics of materials. Such parameters as instrumentation design, specimen characteristics (surface roughness), and the interaction of specimen and environment are of significance in clarifying discrepancies in reported data. Instrumentation design include, among other things, the actual method of measurement (cavities within a specimen or use of a separate blackbody reference), temperature measurement (thermocouple or optical

pyrometer) and degree of temperature control. Specimens are characterized by the surface roughness and chemistry, including the degree of contamination by impurities and oxide layers, and the size and distribution of grains and pores. The specimen environment primarily depends on the method of measurement and can range from vacuum to high pressure, from an inert to a reducing media, or from an inert to a contaminating media. The latter usually occurs when graphite susceptors and carbon reference cavities are used indiscriminately.

Figure 1 shows the total normal emittance of zirconia and chromium oxide coated zirconia measured at three independent laboratories each using a different method. Each source attempted to measure the same parameter (the true total normal emittance) under identical conditions of temperature and pressure. However, source A used a graphite susceptor, a graphite blackbody reference cavity and had a graphite contaminated sample environment causing the high emittance values reported. At the other extreme (low emittance data), source C used a cavity drilled into the specimen as the reference for the temperature measurements. Due to the low thermal conductivity of the material, the cavity temperature was much lower than the surface temperature. In order to test the material at a given temperature the surface temperature had to be much higher than that of the reference cavity, thereby causing evaporation of the coating. This figure illustrates some of the subtle instrumentation characteristics, specimen characteristics, and specimen and environment interactions often overlooked in thermal optical property data generation.

The analysis and correlation of fundamental factors affecting the thermal radiation characteristics will lead to improvements in the accuracy and precision with which reflectance and emittance data can be generated. This in turn can lead to future improvements in the control of reflectance and emittance of new materials being developed for aerospace applications.
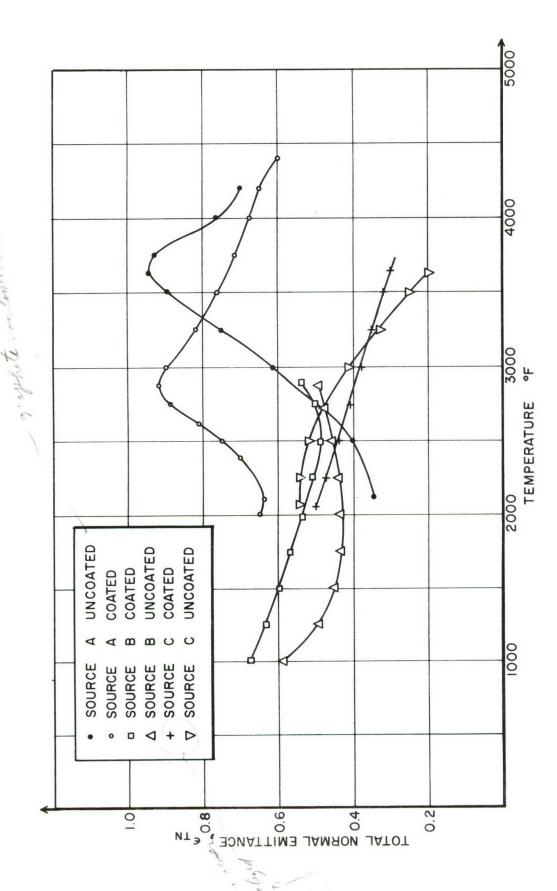
Figure 1. Total Normal Emittance of Zirconia and Chromium Oxide Coated Zirconia

Surfaces are usually defined by two extremes when associated with thermal radiation characteristics, both of which are ideal and not physically obtainable. The first extreme defines a surface as being an optical flat reflector. The second extreme defines a surface as being a perfectly diffuse reflector. Practical surfaces are neither but can approach either one extreme or the other as a limit. The thermal optical properties (emissivity or reflectivity) of a pure, optically flat metal can be determined theoretically with Fresnel relations from the basic optical constants, such as the index of refraction, the absorption coefficient or the angles of incidence and reflection. However, for practical surfaces which are not perfectly flat, the geometry of the interstices can introduce the possibility of interreflections between adjacent areas. Scattering can therefore alter the emission characteristics considerably. Thus, practical measurements determine only the emittance or reflectance of the material.* This geometrical phenomenon introduces another complication into thermal radiation problems. Radiation properties must now be considered not only as a function of the material, the temperature of the radiating surface, and the angle of emission and reflection but for opaque materials, also, as a function of surface roughness.

3. CRITIQUE OF LITERATURE

The study of the interaction of thermal radiation and rough, electrically conducting surfaces is not solely a consequence of space-age problems as implied earlier. In 1901 Rayleigh (Reference 5) made several experimental studies of the relation between the roughness of machined metal and ground-glass surfaces and their effect on the reflection of thermal radiation. Between 1913 and 1916 Coblenz (Reference 6) and Gorton (Reference 7) made rather extensive studies on the reflection of various materials. Three years later Chinmayandam (Reference 8)

took the work of Gorton and derived correlations which showed excellent agreement with experimental data. Additional searches of the literature show many other studies on the interaction of radiation with rough surfaces; however, these studies are primarily extensions of and refinements to the initial fundamental investigations. Beckmann and Spizzichino (Reference 9) have prepared a detailed treatment of the analytical and theoretical approaches used by many investigators.

Several investigators have used related wave phenomena as a model to predict or obtain solutions to the effect of roughness on the reflection of radiation. Davies (Reference 10) studied the reflection of radar from sea waves. He assumed that the surface was a perfect conductor having a peak-to-valley height distribution which was Gaussian. Assuming a perfectly conducting surface eliminates penetration of the electromagnetic radiation and reduces the interaction to a diffraction phenomena. In addition the slopes of the surfaces were assumed to be small so that no shadowing effects were present. He found that the experimental data were consistent with the theory at small angles ($< 40°$) of specular reflection, but showed large discrepancies at large angles. Bennett and Porteus (Reference 11) extended Davies' results by assuming nonperfectly conducting materials. They obtained agreement with Davies' results on surfaces with a root mean square (RMS) roughness of less than 1.27 microns (μ), i.e. the surface irregularities were very small relative to the incident wavelength (greater than about 5μ). They found that when the surface irregularities were comparable in magnitude to the wavelength, the reflectance depended on the surface roughness and the RMS slope. Bennett and Porteus studied only specular reflectance at normal incidence. It is felt, however, that similar studies should include goniometric measurements over the whole hemisphere of

---

*The terminology used in this investigation follows that advocated by Jones and Worthing (References 2 and 3), and accepted for use by the National Bureau of Standards (Reference 4) in that the work-ending "ivity" is reserved for the properties of materials (ideal quantities), and "ance" for the properties of specimens (practical quantities).

reflectance angles since Twersky (Reference 12), in studying polarization effects, discovered that the maximum reflected energy is not necessarily reflected at the specular angle.

Bennett (Reference 13) has also indicated the reason emittance or reflectance changes for a rough surface is not because the surface is rough, but because of the surface damage introduced in the process of making the surface rough. Surface damage refers primarily to the distortion of the crystal lattice by stresses produced in the surface as a result of machining or other surface roughening procedures. Theoretical calculations assume a perfect crystal lattice. However, as a result of surface damage, one no longer has a perfect crystal lattice and the actual optical properties can be very different from the calculated properties. Seban and Rolling (Reference 14) have also noted that surface stress alters the optical constants of a surface. This occurs in such a manner that the reflectance of a metal may correspond to the reflectivity predicted by the Hagen-Rubens Law (Reference 15) in spectral regions (1 to $10\,\mu$) where the law might not be expected to apply. Further evidence by Russell (Reference 16) showed that for copper and stainless steel one effect of the surface stress is to make the distribution of the spectral reflectance similar to that of the Hagen-Rubens Law.

The electron wave functions at or near the surface are very important for any theory of emittance or reflectance of metals, because only the electrons near the surface absorb or emit thermal radiation. Hagen and Rubens (Reference 15), Drude (Reference 17) and Roberts (Reference 18) have unsuccessfully attempted to correlate and predict metallic reflection and absorption in terms of the interaction of classical electromagnetic waves with free and/or bound electrons over the wavelength range of 0.2 to 30μ. However, with more sophisticated quantum mechanical theories it may be possible to almost completely specify the optical properties of certain pure metals in terms of other more easily evaluated solid state parameters such as conductivity-relaxation times and free electron densities (Reference 19).

Even though the nature of the surface conditions and their effects on the thermal radiation characteristics have not been fully explored, and are thus not clearly understood or defined, the differences between real and ideal surfaces can be distinguished (Reference 20) by a highly systematic approach clarifying and categorizing characteristics which give rise to interactions. Gaumer (Reference 21) has adopted a model of an electrically conducting surface which will allow a reasonable prediction of the emittance or reflection of metals. For this model, the important characteristics are the average separation of the peaks, the average height of the peaks, and the average slope of the irregularities. Using such a model, Birkebak, et al. (Reference 22), measured the hemispherical and specular reflectance of nickel surfaces of controlled roughness. Their measurements concluded that the hemispherical reflectance is very sensitive to surface roughness in the range of small roughness values (< 0.2 RMSμ), while for larger roughness values the hemispherical reflectance appears to be relatively insensitive to or independent of the surface roughness. However, the specular reflectance values do continue to decrease with increasing roughness. In many cases the specular reflectance values are more important than total hemispherical reflectance values. As an example, consider a leading edge or nose cap made of a high temperature material which is experiencing a re-entry environment. During re-entry a high temperature shock wave exists which radiates to the leading edge or nose cap at all angles. In a normal direction, the reflectance can be such as to reflect large quantities of the incident heat flux; however, if the surface has characteristics such that the reflected energy is very low in comparison to the incident energy received at large angles from the normal to the surface, the temperature of the material can become quite high.

As a further example, consider a temperature control panel in the side of a system or on a wing of some sort. In the space environment, the control panel radiates to space and, in turn, receives energy flux both directly from the sun and indirectly from other nearby surfaces of the system. Again, the flux received by the temperature control

panel in a direction normal to the surface can probably be handled by the material making up the temperature control panel. Since most optical properties are measured in a direction normal to the surface, it is these values which are used in design calculations. Nevertheless, the solar flux reflected from other parts of the system can be received at angles other than the normal to the surface, and if the material characteristics are such that the reflectance of the panel is greatly dependent upon the viewing angle, the temperature control panel can be rendered useless.

This report considers only one of the above listed specimen characteristics (surface roughness) and its effect on the reflectance of columbium alloy, D-36, pure tantalum and pure tungsten. All other factors have been considered but not studied in systematic detail. A more complete description of the interactions of these other factors with surface roughness and their influence on the optical properties is given in later sections.

These metals and their alloys are becoming more and more important to the aerospace industry because of their high temperature capabilities. Figure 2 shows the useful temperature range of refractory metals; however, oxidation protection coatings will have to be employed to enable the metals to cover the indicated temperature ranges.

Rolling, Funai, and Gaumer (Reference 23) have summarized the thinking of many investigators by stating that the prediction of the thermal radiative characteristics of rough metallic surfaces is a gargantuan task. It necessitates adequate characterization of the surface in terms of its physical and chemical state, backed up by a theoretical understanding of the effect of each and/or a combination of these factors. To date, no such predictions have been made as to the magnitude of these effects. Nevertheless, general trends have been established and some theoretical understanding has been attained in characterizing the radiant properties of rough metallic surfaces.
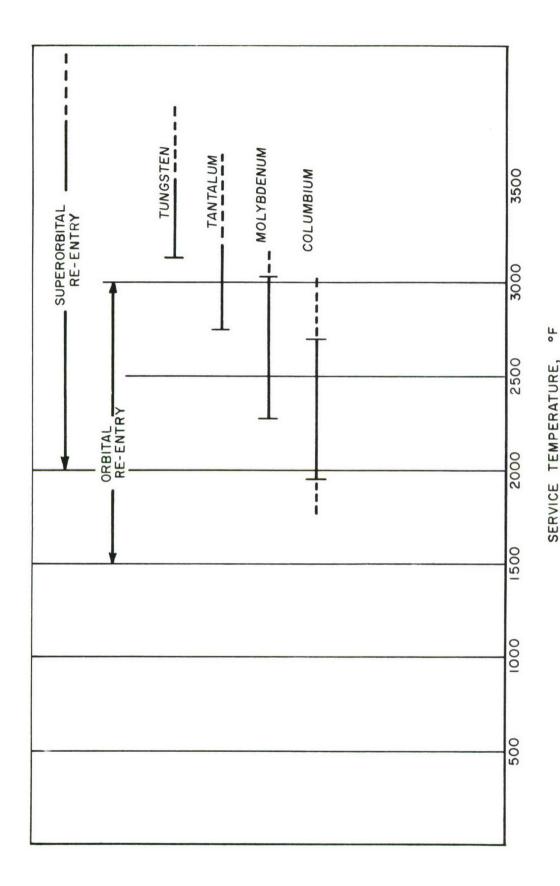
Figure 2. Service Temperature Ranges for Several Refractory Metals

SECTION II

DESCRIPTION OF EQUIPMENT

1. REFLECTION APPARATUS

Figure 3 shows a general view of the reflectance-emittance equipment used in this investigation. Figure 4 is a schematic of the Perkin-Elmer model 13U spectrophotometer and model 205 emittance-reflectance attachment. The model 13U double-beam spectrophotometer is made on a modular or building block philosophy which affords considerable versatility in measurement. For this study the equipment was operated in the double-beam mode (as suggested by Figure 4) using ratio recording for high precision and giving a direct indication of overall instrument sensitivity.

The model 205 attachment is designed to extend the capability of the model 13U to measure the infrared reflectances and emittances of a wide variety of solid samples. Total or diffuse reflectance can be measured over the temperature range of 570° to 2012°F for the incident radiation.

The model 205 attachment, shown schematically in Figure 5, incorporates a heated cavity (hohlraum) which is constructed so as to very closely approach the characteristics of an ideal blackbody radiator over the above temperature range. A sample is inserted into the heated cavity which irradiates it hemispherically and causes it to reflect diffusely. Another area in the cavity is used as a blackbody reference source. The sample and reference beams are made up of these two radiations and are transmitted and focused to the spectrophotometer through a precision optical transfer system. The spectrophotometer compares the two beams at the desired wavelength and accurately records the reflectivity measurement. See Appendix I for Emittance Mode Calibration.

2. TYPES OF MEASUREMENTS

Figure 6 illustrates the three types of reflectances that can be made with this equipment. The upper portion of part A depicts the physical arrangement of the specimen, hohlraum, and detector for total hemispherical reflectance. The lower portion attempts to illustrate what is actually taking place. The specimen is thermally irradiated hemispherically and is viewed by a detector at an angle. In this arrangement the detector senses both the specular and the diffuse components of the radiation reflected by the specimen. This is referred to as total radiation. For normal diffuse reflectance as depicted in part B, the specimen is thermally irradiated hemispherically but viewed normally (in a direction normal to the plane of the specimen's surface). In this case the specular component of the radiation is missing because the aperture in the hohlraum is not radiating to the specimen and the detector senses only a diffuse type of reflectance. To obtain specular reflectance the specimen is placed at mirror position M15 shown in Figure 4. The physical arrangement is shown more clearly in Figure 6, part C. This figure indicates that collimated blackbody radiation irradiates the specimen's surface at an angle of approximately 45 degrees and is detected at the specular angle.

3. HOHLRAUM CAVITY

Three thermocouples are placed at strategic locations to monitor the temperature within the hohlraum cavity. These three thermocouples read the temperature at the top, top side, and lower side of the hohlraum as shown in Figure 7; a temperature controller can sense the temperature of the cavity by any one of the three thermocouples through a selector switch. Automatic "on-off" power cycling controls the temperature of the hohlraum at the value selected on the control dial.

4. SAMPLE HOLDER

Figure 7, also shows a cutaway of the specimen holder. With the specimen in the position indicated by the solid lines normal diffuse reflectancs is measured as described above for case B. When the sample is placed in the holder at an angle indicated by the dotted lines hemispherical reflectance is measured as in case A described above. The specimen is water-cooled from the rear by a mixture of hot and cold water. This allows the specimen temperature to be varied
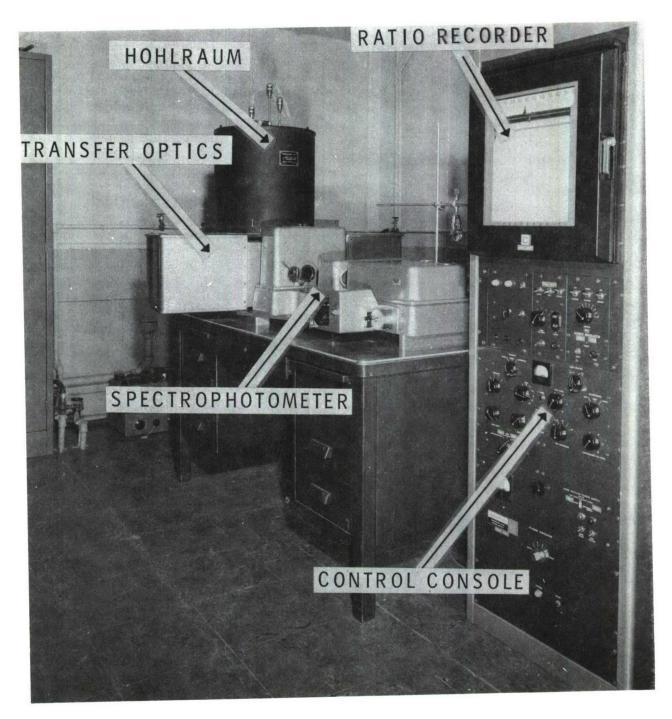
Figure 3. General View of Reflectance-Emittance Equipment
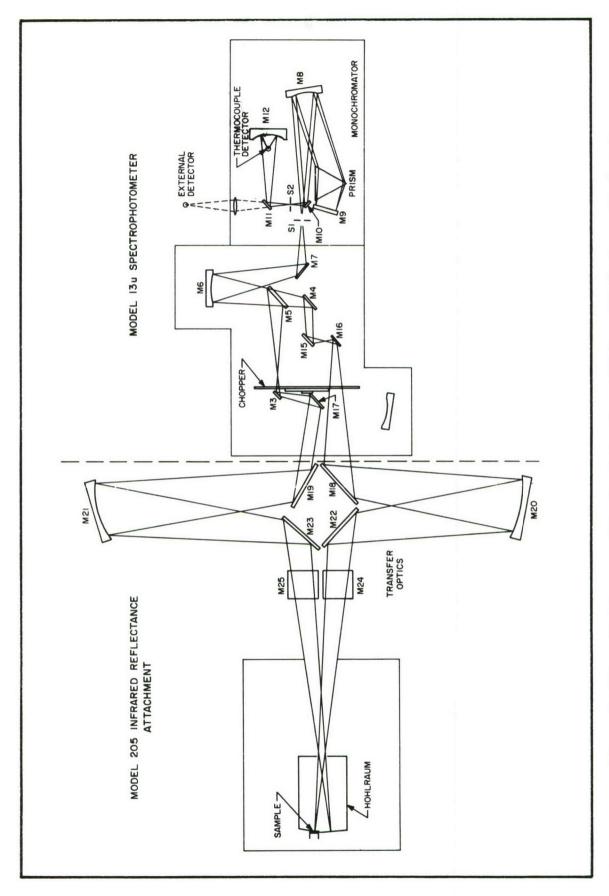
Figure 4. Schematic Diagram of Spectrophotometer and Infrared Reflectance Attachment
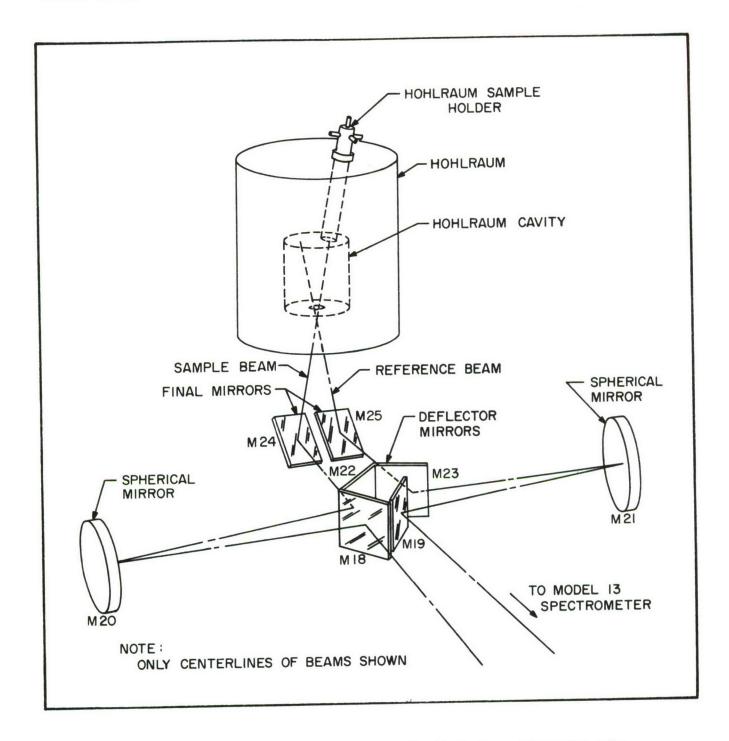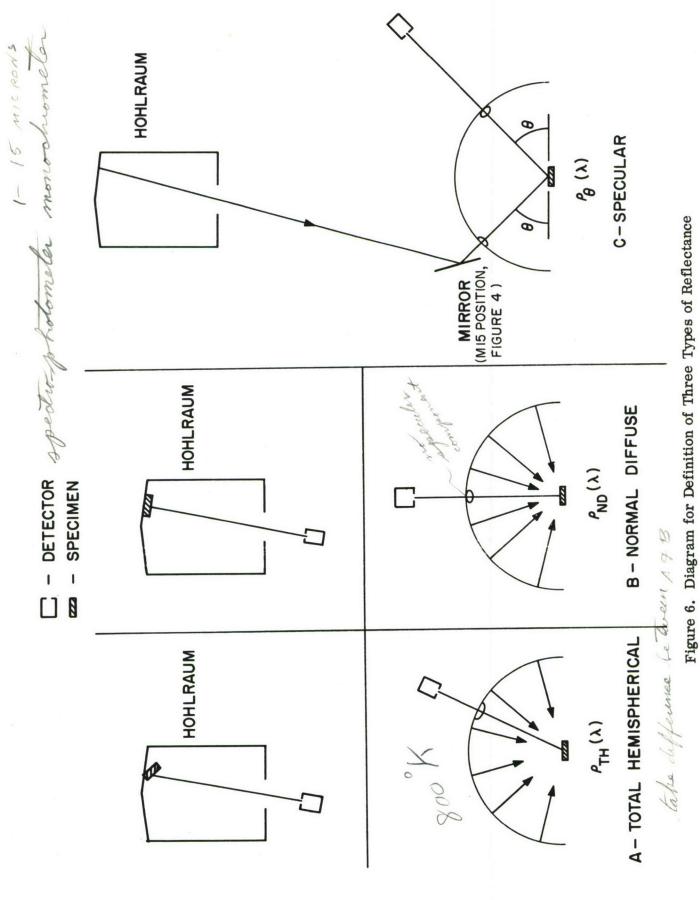
Figure 5. Optical Path to Spectrophotometer for Reflectance Measurements

1— 15 microns

spectro-photometer monochrometer

HOHLRAUM

MIRROR
(M15 POSITION,
FIGURE 4)

$\rho_\theta(\lambda)$

C – SPECULAR

$\square$ – DETECTOR

▨ – SPECIMEN

HOHLRAUM

HOHLRAUM

monochromatic
monochrom

$\rho_{ND}(\lambda)$

B – NORMAL DIFFUSE

HOHLRAUM

$\rho_{TH}(\lambda)$

A – TOTAL HEMISPHERICAL

take difference between A & B

8.00 %

Figure 6. Diagram for Definition of Three Types of Reflectance

Figure 7. Cross Section of Hohlraum

somewhat above and below room temperature by the relative amounts of hot and cold water in the specimen coolant. The specimen is never cooled to the point where condensation forms nor is it heated to the point where its emitted energy is significant.

The sample coolant temperature is monitored by dial thermometers which indicate the coolant temperature before and after contact with the specimen (Reference 24).

5. MONOCHROMATOR

The monochromator shown in Figure 4 is the standard Perkin-Elmer model 83 supplied with the model 13U. For the wavelength range considered in this investigation, the monochromator uses a sodium chloride (NaCl) prism and a thermocouple detector having a window of cesium bromide (CsBr). See Appendix III for Calibration of Spectrophotometer component parts.

6. SURFACE ROUGHNESS MEASUREMENTS

As indicated by Ashby and Schocken (Reference 25) many of the tools needed for proper interpretation of the influence of surface roughness on the thermal radiative characteristics of materials are not generally available. Ideally, the surface roughness should be measured optically without mechanically touching the surface. Once the surface has been touched the surface characteristics can be changed. One would like to measure the reflectance of a material at a certain angle and correlate this measurement to a surface roughness parameter. This study is attempting to make such a correlation and, unfortunately, an independent technique is required to measure the surface roughness.

Stylus instruments are extensively used for surface roughness measurements because of their convenience. However, they have two inherent errors: (1) due to the finite radius of the stylus tip the stylus can not touch the bottom of a sharp valley, (2) the stylus tip can break off the sharp peaks in a soft surface. The peak-to-valley measurements, therefore, can be in error. The surface profiles for this study were recorded by a Taylor, Taylor, and Hobson Talysurf, * model 3, using a stylus for the measurements. Figure 8 gives a general view of the Talysurf. The stylus is a four-sided 90-degree diamond pyramid with a slightly rounded tip about 0.0001-inch wide which bears down on the surface with a force of about 100 milligrams. This low measuring force allows the tracing of all hard materials without visibly marking the surface. The peaks and valleys of the specimen's surface are measured and recorded as the stylus is drawn over the surface. The desired surface parameters can be determined from this recorded trace.

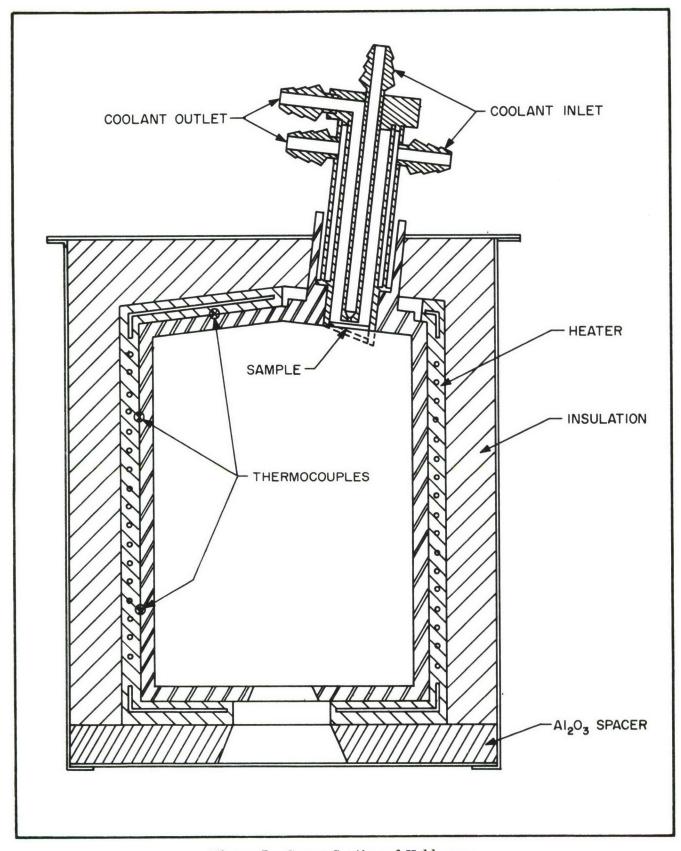Figure 9 indicates the horizontal and vertical measurement characteristics of this instrument. When measuring horizontally there are two speeds with which the stylus can trace a given surface: (1) 11.85 microns per second using a magnification of 100 X, and (2) 59.27 microns per second using a magnification of 20 X. In the vertical direction there are six corresponding magnifications ranging from 0.51 micron per inch to 25.4 microns per inch. For this study the highest magnification which would allow the surface profile trace to remain on the recording chart was used along with the slowest horizontal speed. This provided for higher resolution. In addition to the recorded trace of the surface profile from which Arithmetic Average (AA) peak-to-valley heights were determined,

*Supplied by Engis Equipment Company, Morton Grove, Illinois

the Talysurf features an average meter which provides a Center Line Average (CLA) height of the irregularities of the surface. This instrument makes the following calculation automatically (see Figure 10 for reference):

$$\text{CLA value (microns)} = \frac{a + b + c + \cdots p + q + r + \cdots \ (\text{inches})^2}{L \ (\text{inches}) \ \times \ M} \times 10^6 \ \frac{\text{microinches}}{\text{inch}} \times 0.0254 \ \frac{\text{micron}}{\text{microinch}}$$

where

a,b,c,p,q,r,etc. = areas between the center line and surface profile in inches squared

L = length of a unit surface profile in inches

M = vertical magnification
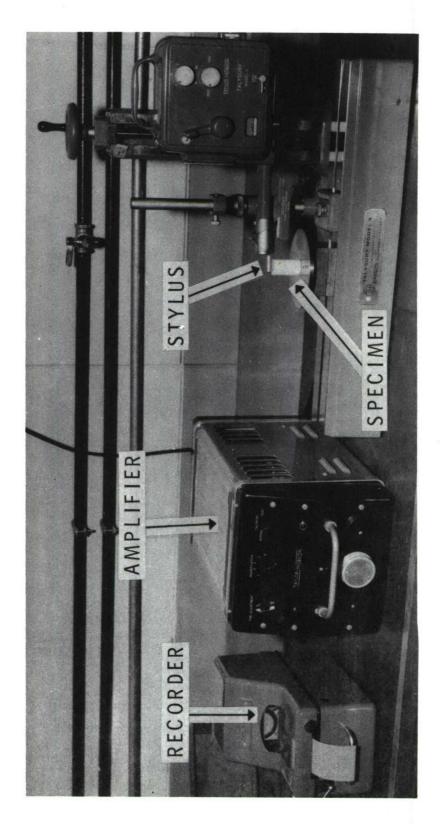
AFML-TR-66-232

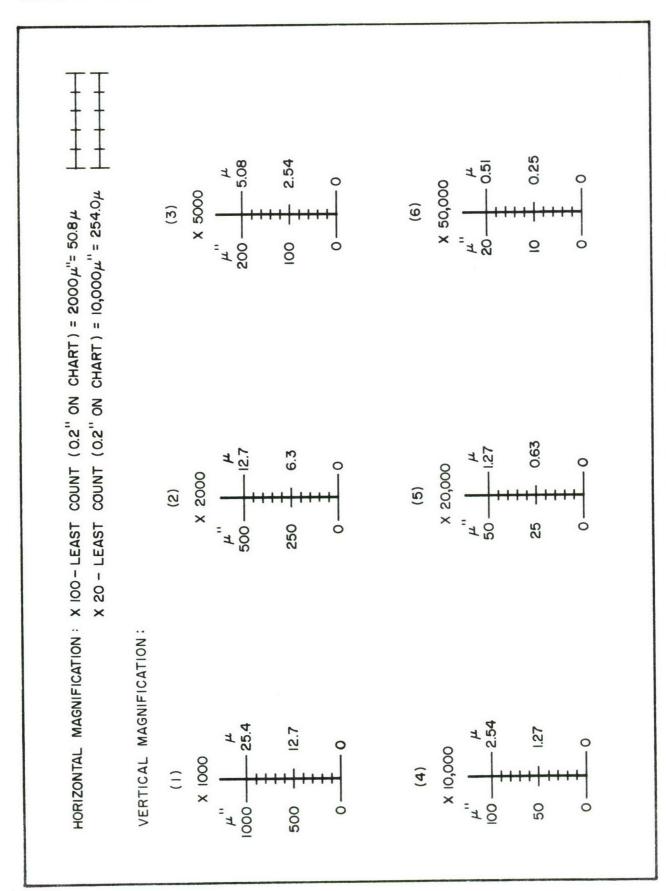Figure 8. General View of Surface Roughness Measuring Equipment

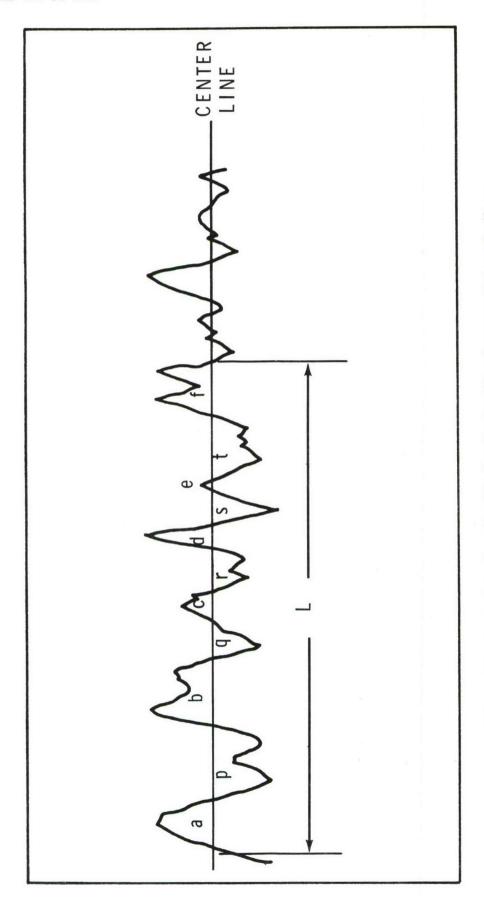Figure 9. Magnification Chart of Surface Roughness Measuring Equipment

16

Figure 10. Typical Surface Profile for Center Line Average Determinations

SECTION III

EXPERIMENTAL PROCEDURE

1. SPECTROGRAPHIC ANALYSIS

Spectrographic analysis was made on a specimen from each type of material. The spectrographic analysis of the columbium alloy, D-36, pure tantalum, and pure tungsten are shown in Table I. The elements that were looked for are listed in column one. The results of the spectrographic analyses are summarized in columns two, three, and four. The columbium alloy, D-36, is 85 percent columbium, with 10 and 5 percent additions of titantium, and zirconium, respectively. No other elements in significant amounts were found. The analysis of the pure tantalum indicated only very small amounts of Cb, Cr, and Fe. None of the other elements looked for was detected. The spectrographic analysis of the pure tungsten specimens indicates that only trace amounts of elements other than tungsten were present.

2. PREPARATION OF SURFACES

a. Random Sanding

All specimens designated by 4/0, 3/0, 2/0, etc., were mechanically sanded to produce a surface having a random lay. Random lay means that the direction of the predominate surface pattern has a random orientation.

All specimens were mechanically sanded in a single direction with 2/0 grit emery polishing paper* until all large scratches or machining marks were removed and only the 2/0 grit marks remained. The samples were then washed in distilled water and air dried. All specimens were turned 90-degrees in the plane of the specimen and were again sanded in a single direction on 3/0 grit emery paper until all 2/0 grit scratch marks were removed. The cleaning procedure was repeated followed by a sanding with 4/0 grit paper. At this point all specimen discs were placed in an automatic vibratory polisher* and polished using 0.05μ grit Al_2O_3 particles.

The 4/0 designation indicates that after the above polishing process was completed the specimen was randomly sanded with the 4/0 grit to produce a random lay surface. The same procedure was followed for the 3/0, 2/0 and 1/0 designations.

b. Sandblasting

All specimens on which the roughness pattern was to be developed were lapped to a flatness of ten millionths of an inch.

The following procedures were used to develop these random lay roughness patterns.

(1) 10 μ inch RMS Finish: A very fine 100 grit sand was dispersed in water with the resulting mixture forced out of a nozzle under high pressure. The "vapor" stream produced was directed onto the specimen surface, short lapping operation followed.

(2) 40 μ inch RMS Finish: The surface was sandblasted with the same fine silica sand followed by a short lap.

(3) 80 μ inch RMS Finish: The surface was sandblasted with the same fine silica sand at a location closer to the high pressure spray nozzle.

(4) 120 μ inch RMS Finish: The surface was sandblasted with a coarser silica sand.

c. Cleaning Surfaces

All specimens were vigorously washed in soap and cold water with a rinse of acetone. Each specimen was ultrasonically cleaned in methanol for several hours to remove any

*Supplied by Buehler LTD. Evanston, Illinois

*Manufactured by the Syntron Company, Homer City, Pa.

TABLE I

SPECTROGRAPHIC ANALYSIS OF

SPECIMENS

ELEMENT	COLUMBIUM ALLOY, D-36	PURE TANTALUM	PURE TUNGSTEN
Al	Tr*	ND	<0.0006%
B	ND*	ND	ND
Ca	Tr	ND	<0.0003%
Cb	85%	0.02%	ND
Cr	ND	0.002%	<0.0003%
Cu	Tr	ND	0.0005%
Fe	Tr	0.01%	0.0005%
Mg	Tr	ND	<0.0003%
Mn	ND	ND	<0.0006%
Mo	ND	ND	0.0028%
Ni	ND	ND	0.0004%
Si	Tr	ND	<0.0007%
Sn	ND	ND	<0.0006%
Ta	Tr	Bal*	ND
Ti	10%	ND	ND
V	ND	ND	ND
W	ND	ND	Bal
Zr	5%	ND	ND
Oxygen	NL*	NL	7±5PPM*
Nitrogen	NL	NL	1±1PPM
Hydrogen	NL	NL	1±1PPM
Carbon	NL	19PPM	<10PPM

* Tr   - Trace
  ND   - Not Detected
  NL   - Not Looked For
  PPM - Parts Per Million (1PPM = 0.0001%)
  Bal. - Balance of Material

foreign particles that may have become embedded in the interstices of the surface. The specimens were then air dried. Microscopic examination revealed there was no foreign material imbedded in the surfaces.

3. SURFACE ROUGHNESS MEASUREMENTS

Surface roughness profiles for the columbium alloy, D-36, pure tantalum, and pure tungsten are shown in Figures 11 through 18. In some cases the mean line of the surface had a slope because the specimen's bottom surface was not parallel to the top surface or was not flat. This caused the recorder trace to drift up or down depending on the slope of the mean line.

The peak-to-valley height of each trace was measured by an optical comparator having 250 divisions per inch. The average value of the forty peaks read was used to provide the data in Table II. In column 7 the micron values for 40, 80, and 120 μ inch RMS values were converted by a direct calculation to change micro inches to microns, plus an 11 percent correction to change the RMS values to Arithmetic Average (AA) values (Reference 26). The decision to measure a particular peak-to-valley ratio was somewhat arbitrary being, in general, based upon whether its spacing agreed with the regularity of the overall trace. Measurements were made only on predominate peaks, but again the judgment concerning predominant or primary and secondary peaks was somewhat arbitary. In addition to the AA and CLA surface roughness values, the optical surface roughness for each material was calculated using equations derived by Bennett and Porteus (Reference 11). This data is shown in column 9 of Table II.

4. REFLECTANCE MEASUREMENTS

The three types of reflectances explained earlier were measured for each metal and surface condition. Meticulus care was exercised in handling the specimens after cleaning and during each measurement.

For each measurement 100 and 0 percent reference lines were determined. For the 100 percent reference the radiation from the hohlraum was sent through both optical paths of the spectrophotometer. For the 0 percent reference no energy was sent through the sample path while the reference radiation from the hohlraum was sent through the reference optical path.

The specimen was placed in the sample holder and cooled to room temperature with cooling water. The hohlraum temperature was maintained at 980°F (527°C) throughout all measurements. The reflected energy from the cooled specimen was sent through the sample path and detected by the monochromator.

Two sample holders were used in making the reflectance measurements. One sample holder tilts the specimen at an angle of 20 degrees to the normal of the sample beam to give total reflectance. The other places the sample normal to the sample beam to give normal diffuse reflectance. To measure the specular reflectance the specimen was placed at the mirror position M-15 shown in Figure 4.

The heights of the respective curves are measured at preselected wavelengths and the reflectance is computed for each wavelength. If Z_λ is the height of the "0% line" (where all measurements are in arbitrary units), S_λ the height of the "specimen line" and H_λ the height of the "100% line," at the same wavelength, λ, the reflectance, $\rho(\lambda)$, is given by

$$\rho(\lambda) = \frac{S_\lambda - Z_\lambda}{H_\lambda - Z_\lambda}$$

Values of $\rho(\lambda)$ are computed for each preselected wavelength in the range of 1.88 to 13.3 μ, and $\rho(\lambda)$ plotted as a function of wavelength. A curve drawn through the plotted points represents the spectral reflectance of the specimen.
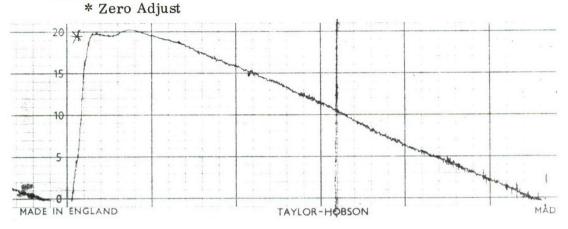
TABLE II

SURFACE CHARACTERISTICS OF SPECIMENS

ρ_{TH}
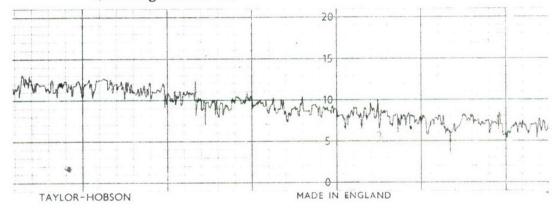
SPECIMEN	SURFACE PREP-ARATION	DT** → SYMBOL → λ*** →	15.57 • 1.88	14.07 X 4.99	10.45 O 9.05	5.00 Δ 12.8	PEAK-TO-VALLEY HEIGHT (MICRONS) MEASURED AA σ_m	CLA σ_m	OPTICAL ρ σ_o
COLUMBIUM ALLOY, D-36	4/0		0.617	0.770	0.858	0.910	0.163		0.232
	3/0		0.571	0.718	0.809	0.880	0.592		0.302
	2/0		0.480	0.637	0.751	0.830	0.775		0.373
	10RMS		0.430	0.511	0.651	0.737	0.988		0.525
	10RMS		0.425	0.501	0.579	0.621	1.015*		0.676
	40RMS								
TANTALUM	4/0		0.711	0.830	0.891	0.933	0.192	0.104	0.210
	3/0		0.630	0.753	0.847	0.903	0.450	0.178	0.309
	2/0		0.626	0.746	0.833	0.886	0.588	0.312	0.331
	10RMS		0.570	0.650	0.736	0.800	0.698	0.341	0.470
	40RMS		0.500	0.572	0.639	0.705	1.015*	1.623	0.593
	120RMS		0.440	0.533	0.619	0.685	3.045*	3.917	0.605
TUNGSTEN	3/0		0.882	0.955	0.974	0.970	0.065		0.143
	2/0		0.858	0.949	0.971	0.983	0.147		0.033
	10RMS		0.510	0.688	0.812	0.888	0.737		0.341
	40RMS		0.580	0.700	0.758	0.797	1.015*		0.480
	80RMS		0.570	0.705	0.784	0.834	2.030*		0.430

*DIRECT CONVERSION FROM RMS MICROINCHES TO AA MICRONS
**INDICATES DRUM TURNS SYMBOL. THESE SYMBOLS ARE USED IN FIGURES OF SURFACE ROUGHNESS
***WAVELENGTH IN MICRONS

1. Vertical Magnification: X 50,000
   Horizontal Magnification: X 100
   Polished D-36
      * Zero Adjust

2. Vertical Magnification: X 20,000
   Horizontal Magnification: X 100
      4/0 Roughened D-36

3. Vertical Magnification: X 20,000
   Horizontal Magnification: X 100
      3/0 Roughened D-36
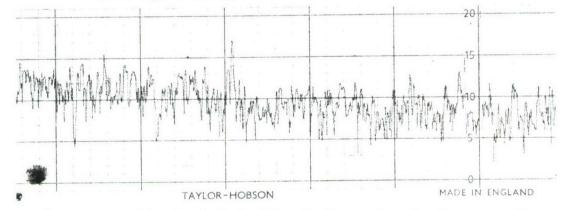
Figure 11. Surface Profile of Polished, 4/0 and 3/0 Roughened Columbium Alloy, D-36

4.   Vertical Magnification: X 10,000
       Horizontal Magnification: X 100
              2/0 Roughened D-36

5.   Vertical Magnification: X 10,000
       Horizontal Magnification: X 100
              1/0 Roughened D-36

Figure 12. Surface Profile of 2/0 and 1/0 Roughened Columbium Alloy, D-36

6.   Vertical Magnification: X 10,000
        Horizontal Magnification: X 100
          10 RMS Roughened D-36

7.   Vertical Magnification: X 5,000
        Horizontal Magnification: X 100
          40 RMS Roughened D-36

8.   Vertical Magnification: X 2,000
        Horizontal Magnification: X 100
          120 RMS Roughened D-36
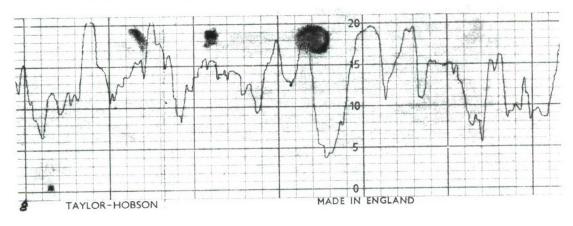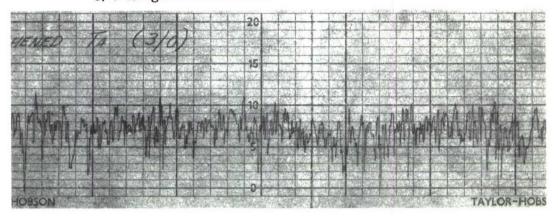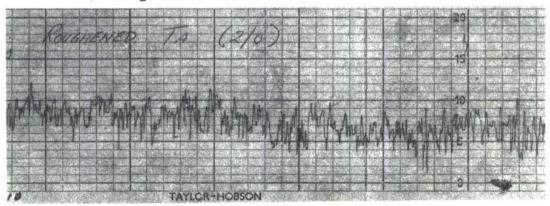
Figure 13. Surface Profile of 10, 40 and 120 RMS Roughened Columbium Alloy, D-36

9. Vertical Magnification: X 20,000
    Horizontal Magnification: X 100
    3/0 Roughened Tantalum

10. Vertical Magnification: X 10,000
     Horizontal Magnification X 100
     2/0 Roughened Tantalum

11. Vertical Magnification: X 10,000
     Horizontal Magnification: X 100
     1/0 Roughened Tantalum
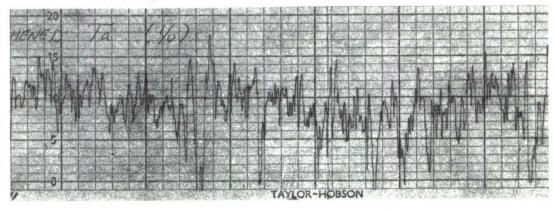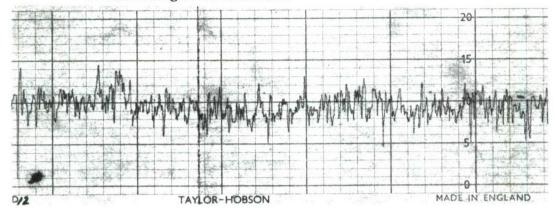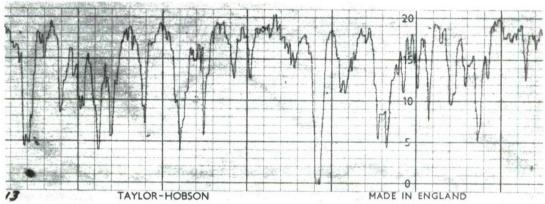
Figure 14. Surface Profile of 3/0, 2/0, and 1/0 Roughened Tantalum

12. Vertical Magnification: X 10,000
    Horizontal Magnification: X 100
       10 RMS Roughened Tantalum

13. Vertical Magnification: X 5,000
    Horizontal Magnification: X 100
       40 RMS Roughened Tantalum

14. Vertical Magnification: X 2,000
    Horizontal Magnification: X 100
       120 RMS Roughened Tantalum

Figure 15. Surface Profile of 10, 40 and 120 RMS Roughened Tantalum

15.   Vertical Magnification: X 50,000
        Horizontal Magnification: X 100
        Polished Tungsten
          * Zero Adjust

16.   Vertical Magnification: X 50,000
        Horizontal Magnification: X 100
          4/0 Roughened Tungsten

17.   Vertical Magnification: X 50,000
   Horizontal Magnification: X 100
          3/0 Roughened Tungsten
          * Zero Adjust

Figure 16. Surface Profile of Polished, 4/0 and 3/0 Roughened Tungsten

AFML-TR-66-232

18. Vertical Magnification: X 20,000
Horizontal Magnification: X 100
2/0 Roughened Tungsten

19. Vertical Magnification: X 20,000
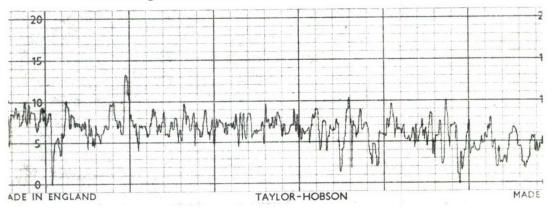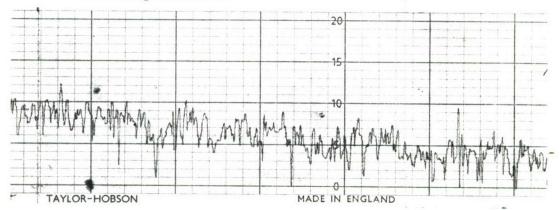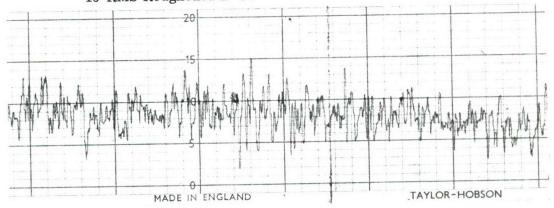Horizontal Magnification: X 100
1/0 Roughened Tungsten

Figure 17. Surface Profile of 2/0 and 1/0 Roughened Tungsten

20.   Vertical Magnification: X 10,000
        Horizontal Magnification: X 100
           10 RMS Roughened Tungsten

21.   Vertical Magnification: X 5,000
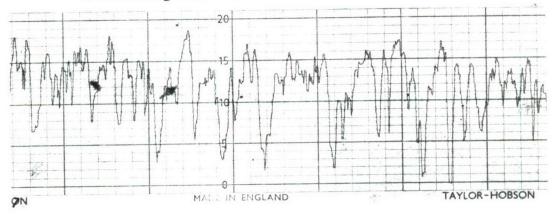   Horizontal Magnification: X 100
           40 RMS Roughened Tungsten

22.   Vertical Magnification: X 2,000
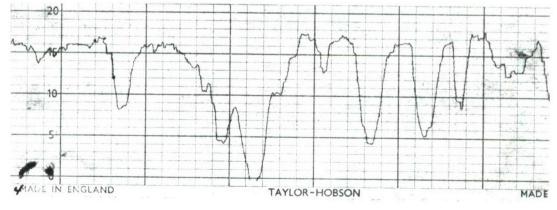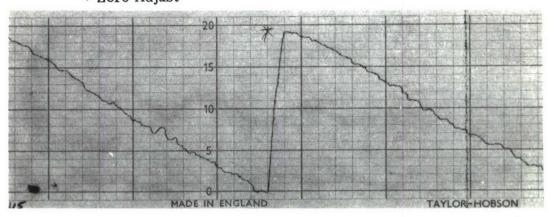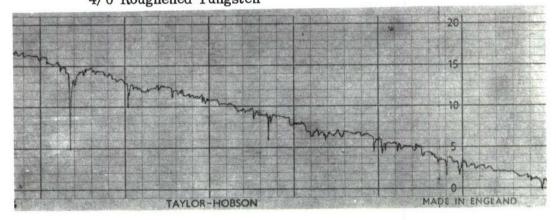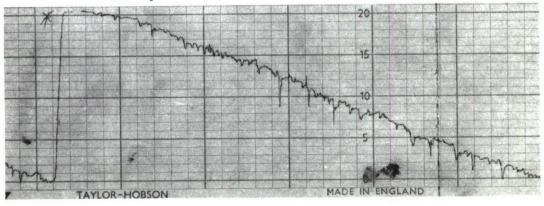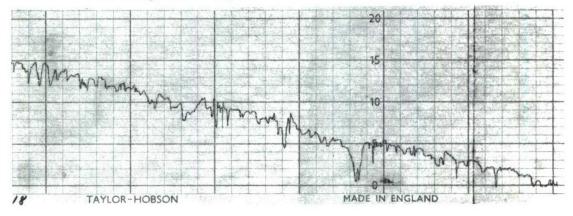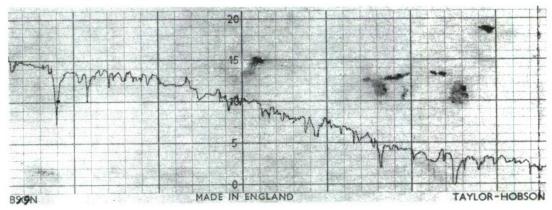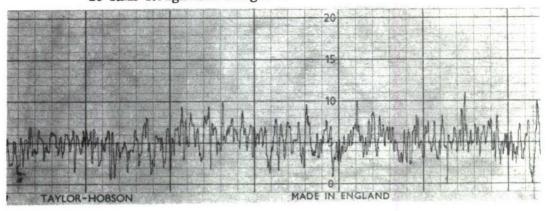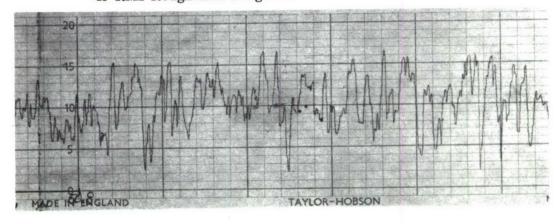   Horizontal Magnification: X 100
           80 RMS Roughened Tungsten
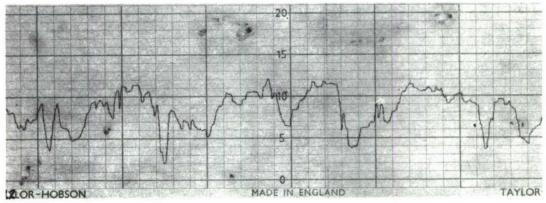
Figure 18. Surface Profile of 10, 40 and 80 RMS Roughened Tungsten

SECTION IV

RESULTS

As indicated above, Table II is a summary of the suface roughness profiles and reflectance measurements. The average peak-to-valley heights for any one material seem to be fairly consistent with the preparation technique in that they increase with increasing roughness except for the 3/0 and 2/0 surfaces of tungsten which appear low. This, however, can be attributed to the hardness of the metal. The 10, 40, 80 and 120 RMS surfaces were prepared by sandblasting techniques and their RMS values were directly converted to AA in microns. This direct conversion was necessary because the peak-to-valley heights (except for the 10 RMS surfaces) generally were too large to be measured accurately by the optical comparator technique.

1. COLUMBIUM ALLOY, D-36

Figure 19 shows the total hemispherical reflectance of the columbium alloy, D-36, as a function of roughness and wavelength. The numbers beside each curve are the surface roughness values from Table II. These curves illustrate two things:

(1) As the surface becomes smoother the total hemispherical reflectance becomes higher at any particular wavelength, and

(2) As the wavelength of the reflected energy is increased the reflectance becomes higher due to the apparent smoothing of the surface. In this case the long wavelengths do not "see" the roughness of the surface. Figure 20 illustrates this phenomenon. In Part A the wavelength of incident radiation is of the same order of magnitude as the surface roughness profile, and the incident energy is reflected in many directions due to reflections from the sides of the peaks and valleys in the surface. In the case where the wavelength is much greater than the surface roughness, as in Part B, the incident energy is reflected in the specular direction. Thus, practically all of the incident energy is received at a detector placed in the specular direction and, consequently, the reflectance is much higher in this case than for the case

illustrated in Part A where a large portion of the energy was reflected in directions other than the specular direction.

The specular reflectance is plotted as a function of wavelength for a set of surfaces in Figure 21. Note that the rough surface of the 120 RMS (3.045AA μ) curve has a low reflectance due to its being very diffuse and thereby scattering the reflected flux in many directions so that much of the energy is lost in the specular direction. The 10 RMS (0.988 AA μ) curve appears to be a transition type surface. At short wavelengths the reflected flux is diffuse and the reflectance very low, while at the long wavelengths the surface appears smoother and a much larger quantity of energy is reflected at the specular angle making the reflectance much higher for longer wavelengths. The curves for the 0.592 and 0.775 AA micron surfaces show the increase in reflectance due to the smoother surfaces.

The total hemispherical reflectance was plotted as a function of the surface roughness, σ_m, measured in AA microns at several wavelengths as shown in Figure 22. The curves show a discontinuity around a surface roughness of 1AA μ for wavelengths greater than approximately 5 μ. The reflectance values of the 120 RMS surface suggested the data smoothed out beyond 1.0 AA μ surface roughness. This suggests that the total hemispherical reflectance follows one function of the surface roughness between 0.1 and 1.0 AA μ and another function for surface roughness beyond 1.0 AA μ. This phenomenon can be attributed to the fact that the method of surface preparation was different in the two ranges (random sanding between 0.1 and 0.9 AA μ and sandblasting beyond 0.9 AA μ). Thus, the surface energy or stress of the surface can be different and lead to two different functional relationships.

2. TANTALUM

Figure 23 illustrates the effect of roughening the surface of tantalum to various degrees.

The total hemispherical reflectance of tantalum is increased as the surface is made smoother or less diffuse. This data shows that without a proper description of the surface or characteristic surface roughness parameter, the reflectance can range from approximately 0.45 to 0.70 reflectance units at 2 μ, and approximately 0.68 to 0.93 reflectance units at 13 μ.

The normal diffuse reflectance is plotted as a function of wavelength for several roughened surfaces of tantalum in Figure 24. In this illustration the rougher surface has the higher reflectance since, in the technique of measuring the normal diffuse component, more reflected flux is received at the detector from a diffuse surface than a specular surface. As indicated earlier, very little energy is received in the detector for a specular surface since there is an aperture in the hohlraum in the specular direction for this measurement. Thus, smooth or specular surfaces such as a 0.192 AA μ surface have a very small normal diffuse reflectance component, while rough surfaces (1.015 and 3.045 AA μ surfaces) have a large normal diffuse reflectance. The 10 RMS (0.6553 AA μ) curve again illustrates a transition type surface from 2 to 13 μ.

This point is dramatically illustrated in Figure 25. In this figure the specular reflectance is plotted as a function of wavelength for the same surfaces as in Figure 23. Again it can be seen that for the rough surfaces the specular reflectance is very low; however, as the wavelength increases the specular reflectance increases as the surface becomes smoother for the longer wavelengths. The 0.698 AA μ surface appears as a transition surface ranging from a low specular reflectance surface at short wavelengths to a highly specular surface at long wavelengths in the infrared region. The smoother surface, 4/0 (0.192 AA μ), appears to be a transition surface for wavelengths in the long wavelength visible and near infrared regions. This is illustrated between 2 and 5 μ where the curve drops considerably. For the longer wavelengths in the infrared the surface has a high specular reflectance. In Figures 26, 27 and 28 the total hemispherical reflectance of tantalum is plotted as a function of the surface roughness in microns at several wavelengths. In Figure 26 a "hump" is indicated

in the curves at approximately 0.6 AAμ surface roughness. This again suggests the dual functionality of the total hemispherical reflectance in relation to the surface roughness as explained for the columbium alloy, D-36. This point is further demonstrated in Figure 27. The difference between these two figures lies in the description of the surface. The Arithmetic Average surface roughness is plotted in Figure 26 and the Center Line Average surface roughness in Figure 27.

A comparison of the two figures shows that for the AA surface description the large values of surface roughness are compressed, whereas, the small values are spread out. The opposite holds for the CLA description causing an enhancement of the hump in the previous figure.

Additional studies are being made on these materials. In order to determine if surface stresses have caused such phenomena as indicated, the specimens are being annealed in a reducing atmosphere to relieve these stresses.

Birkebak, et al. (Reference 22), have indicated that beyond a certain surface roughness, the hemispherical reflectance may be independent of further increases in roughness. However, Birkebak's data extends to a surface roughness of only about 1.0 μ. The data in Figures 26 and 27 extend to approximately 3 μ and show a slight decrease, i.e., the total hemispherical reflectance is not completely independent of the surface roughness. This decrease is probably due to the peak-to-valley slopes which can be quite large in this extreme roughness case and cause specular reflections from the slopes. Other second order effects, such as differences in surface energies, can also cause this decrease.

In Figure 28 the total hemispherical reflectance was again plotted as a function of the surface roughness, but this time the surface roughness, σ_0 was determined optically using the method suggested by Bennett (Reference 11). An optical method of describing a surface is felt to be more accurate in that it considers all secondary effects such as shadowing and surface stresses. However, the magnitudes of the secondary effects cannot be evaluated by Bennett's method since

his equation does not account for these effects. For the optical surface roughness the total hemispherical reflectance appears to be a second order functional relationship for wavelengths larger than $9.0\,\mu$. At shorter wavelengths the curves appear to become functions of higher order which might be caused by the dispersion of the optics in the measuring instrument, and the assumptions used in deriving Bennett's equation, i.e., σ/λ must be small, indicating the equation only holds for long wavelengths. This method of measuring the surface roughness is being studied further and will be reported at a later date.

3. TUNGSTEN

Figure 29 shows the total hemispherical reflectance as a function of wavelength for tungsten having several values of surface roughness. The curves for 0.065 and 0.147 AA μ roughened surfaces are practically the same except at shorter wavelengths where the smoother surface shows a slightly higher reflectance. Tungsten is so hard that there is only a small difference in surface roughness produced by the two preparation techniques. A greater surface roughness is produced by sandblasting as in the case for the lower two curves, but even with this procedure there is only a maximum difference of 6 percent in reflectance. The cross-over of the 1.015 and 2.030 AA micron curves at 6.7 microns may be attributed to the second order effects of the peak-to-valley slopes. Because of the hardness of tungsten the sides of the rougher surface with high peak-to-valley ratios have smooth slopes which contribute more to the reflectance at wavelengths shorter than 6.7 microns.
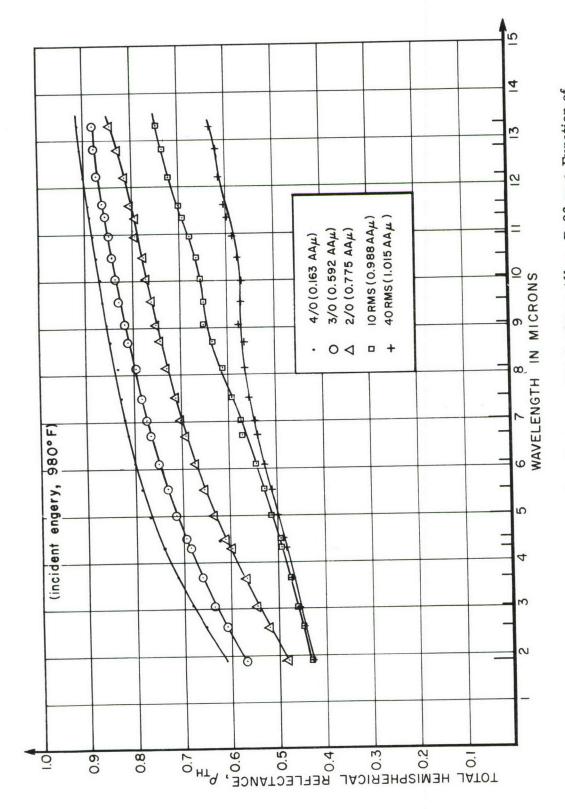
In Figure 30 the specular reflectance is plotted as a function of wavelength for tungsten having several surface roughness values. This figure illustrates the fact that unless some indication is given of the surface roughness value, the specular reflectance can range from 0.01 to practically 1.0. The curve designated 3/0 (0.065 AA μ) is practically a mirror surface, thus the specular reflectance values approach 1.0 very closely. The reason for the drop in reflectance beyond 11μ is unexplained. Again it appears that the 0.737 AA μ surface is a transition type surface for tungsten.

Figure 31 compares the total hemispherical reflectance as a function of wavelength for the three metals studied in this investigation. The surface roughness of each metal was approximately the same (0.14 to 0.19 AA μ). This figure shows the material effects on the reflectance independent of surface roughness. Figure 32 is a similar plot; however, the surfaces are much rougher (0.69 to 0.77 AA μ). In both figures tungsten has the higher total hemispherical reflectance, except in Figure 32 where tungsten drops slightly below tantalum at $3.5\,\mu$. The total hemispherical reflectance of tantalum is higher than the columbium alloy, D-36, in both figures throughout the wavelength range (2 to $13\,\mu$).

A comparison of Figures 19, 23, 29, and 32 indicates that of the materials studied, there was an average difference in the reflectance of only 16 percent or less, whereas roughening the surface of the same material caused deviations in the total hemispherical reflectance for the columbium alloy, D-36, ranging from 20 to 27 percent, for tantalum from 24 to 27 percent, and for tungsten from 15 to 37 percent.

In Figure 33 the total hemispherical reflectance of all three materials was plotted as a function of the optical surface roughness. It appears that a plot of this type is independent of material effects. Bennett and Porteus (Reference 11) have indicated that the wavelength control of the reflectance measuring spectrophotometer can be calibrated so that roughness values can be read directly from the wavelength setting. The data in Figure 33 indicates this to be the case with the added information that the technique appears to be material insensitive and will not require a separate calibration for each material being studied.

Figure 19. Total Hemispherical Reflectance of Columbium Alloy, D-36 as a Function of Wavelength

REFLECTED

INCIDENT

PART B

LONG WAVELENGTH MUCH
GREATER THAN SURFACE
ROUGHNESS PROFILE

REFLECTED

INCIDENT

REFLECTED

ROUGH
SURFACE

PART A

SHORT WAVELENGTH SAME
MAGNITUDE AS SURFACE
ROUGHNESS PROFILE
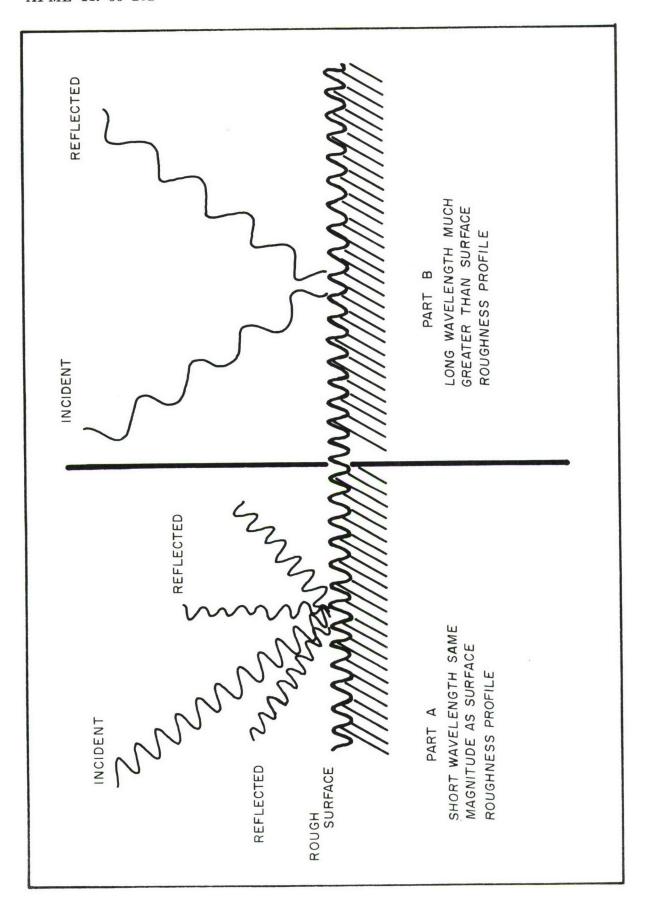
Figure 20. Comparison of the Interaction of Short and Long Wavelength Radiation With a
Rough Surface
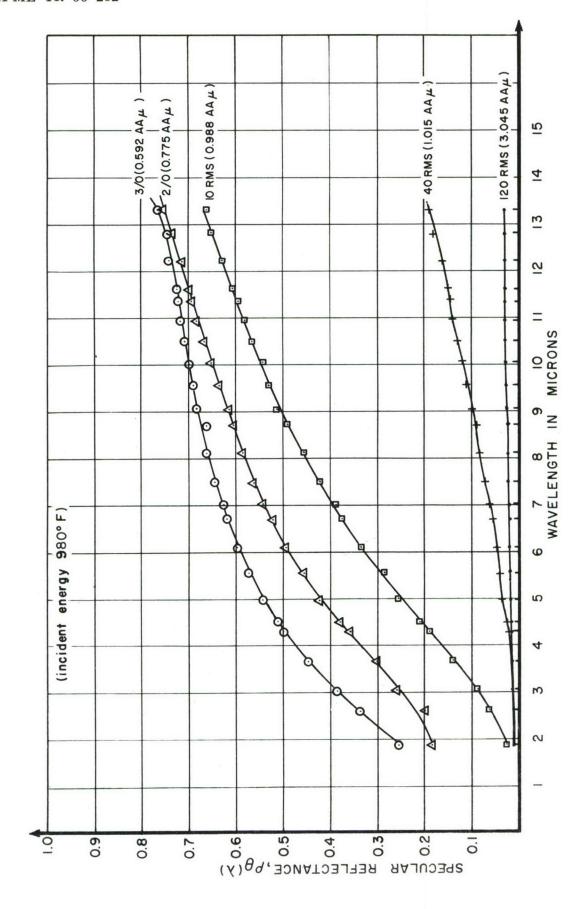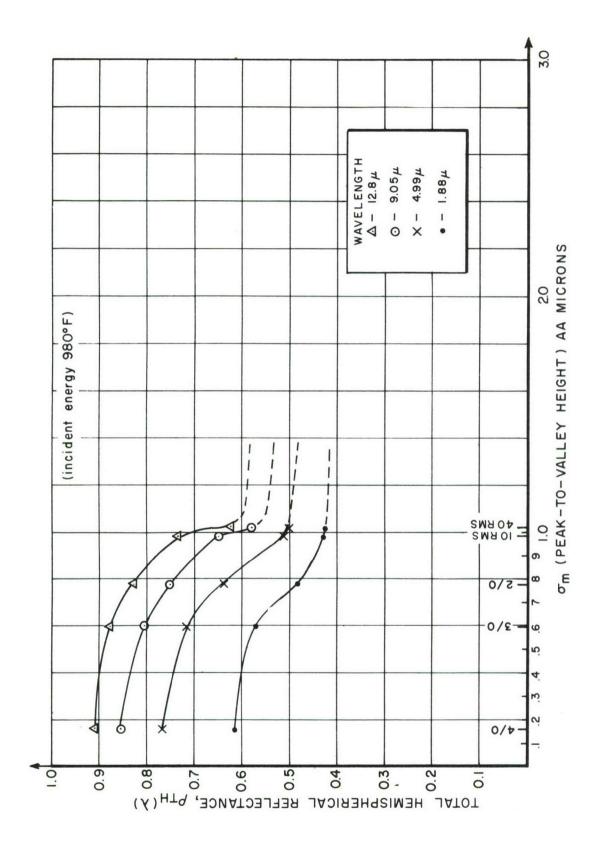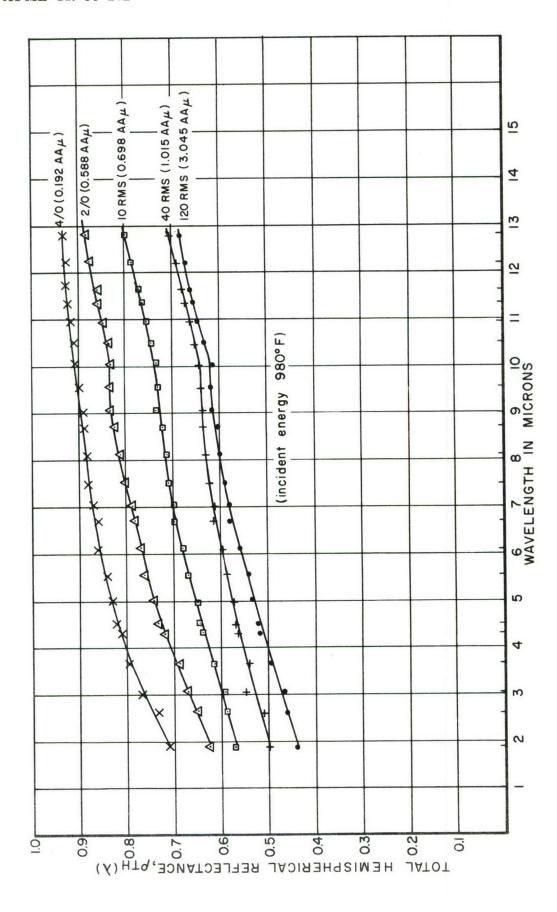
Figure 21. Specular Reflectance of Columbium Alloy, D-36, as a Function of Wavelength

Figure 22. Total Hemispherical Reflectance of Columbium Alloy, D-36, as a Function of the Mechanical Surface Roughness

Figure 23. Total Hemispherical Reflectance of Tantalum as a Function of Wavelength
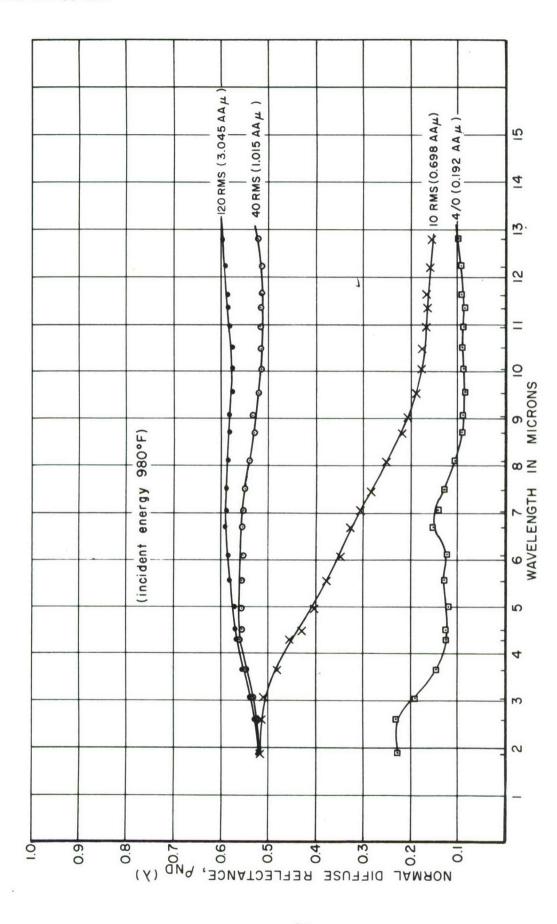
Figure 24. Normal Diffuse Reflectance of Tantalum as a Function of Wavelength
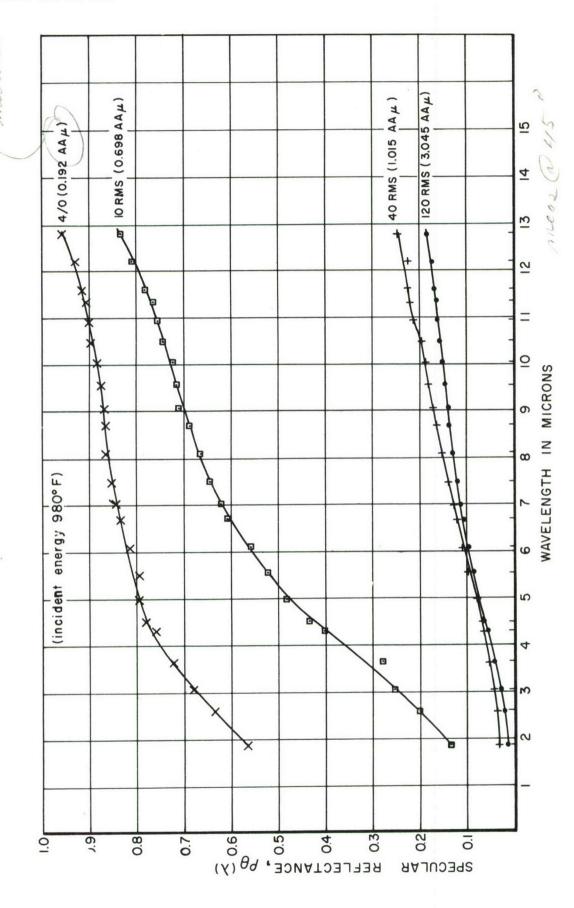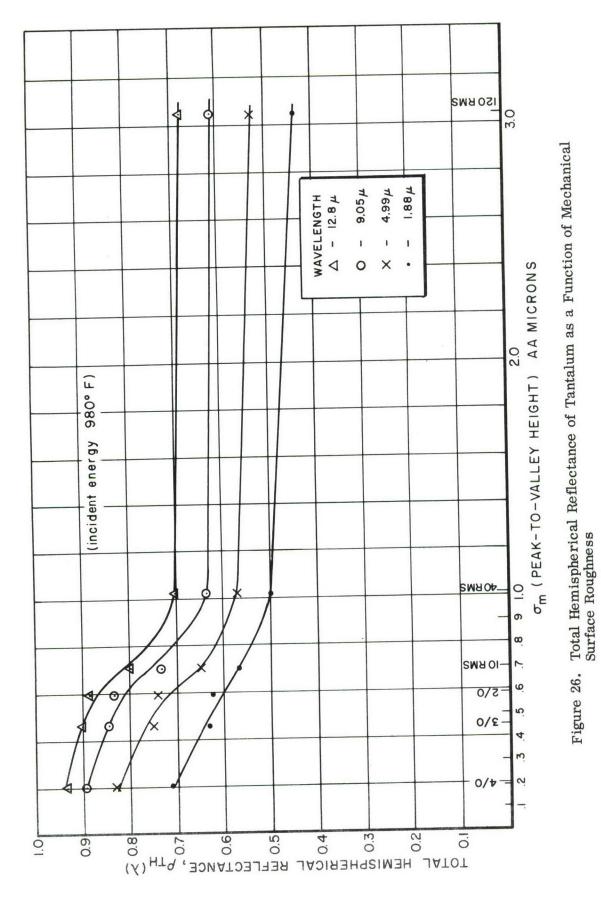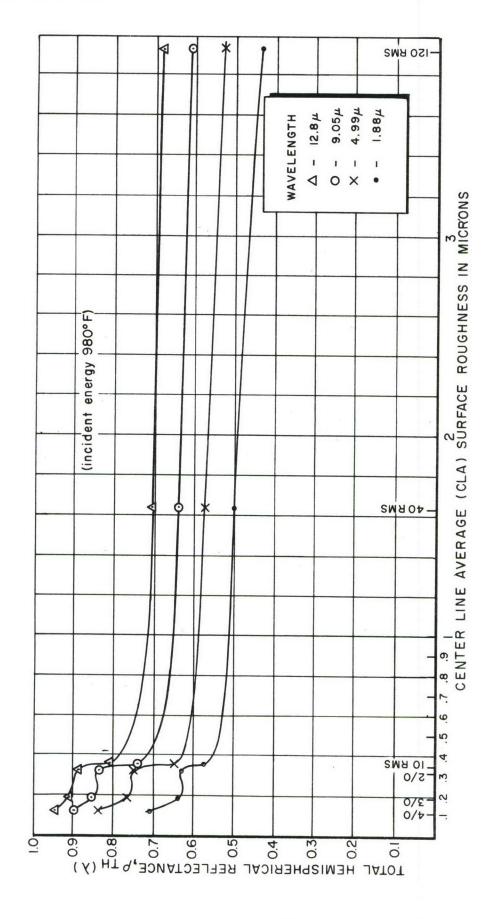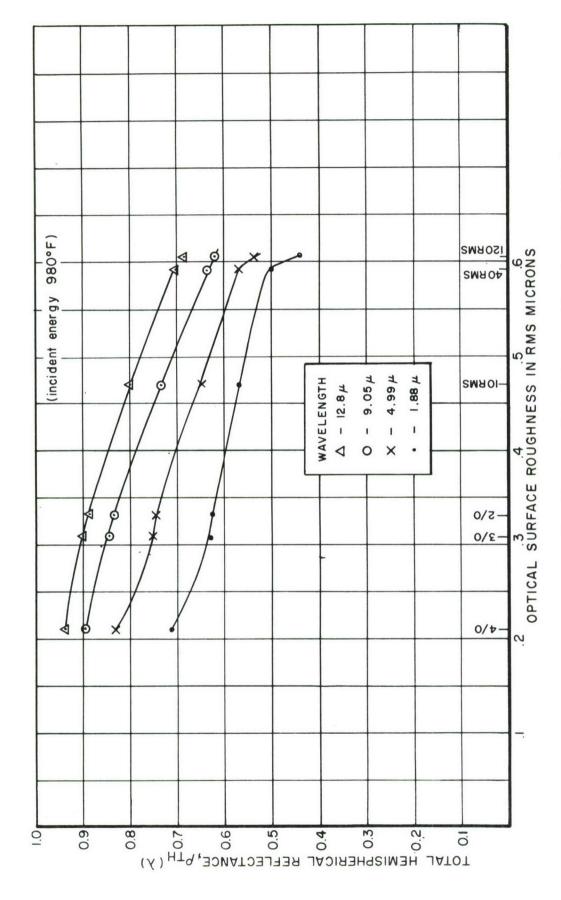
Figure 25. Specular Reflectance of Tantalum as a Function of Wavelength

Figure 26. Total Hemispherical Reflectance of Tantalum as a Function of Mechanical Surface Roughness

Figure 27. Total Hemispherical Reflectance of Tantalum as a Function of the Center Line Average Surface Roughness

41

Figure 28. Total Hemispherical Reflectance of Tantalum as a Function of the Optical Surface Roughness
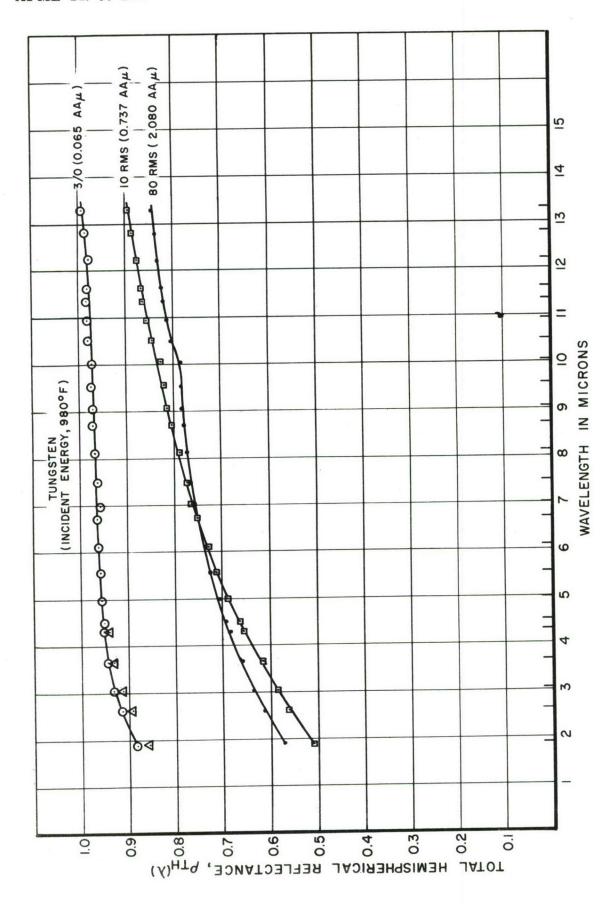
Figure 29. Total Hemispherical Reflectance of Tungsten as a Function of Wavelength
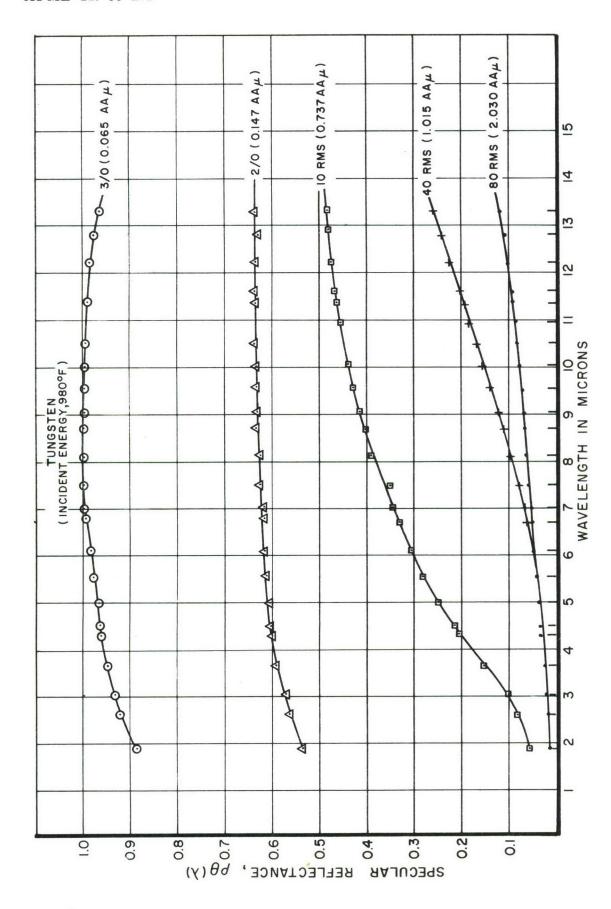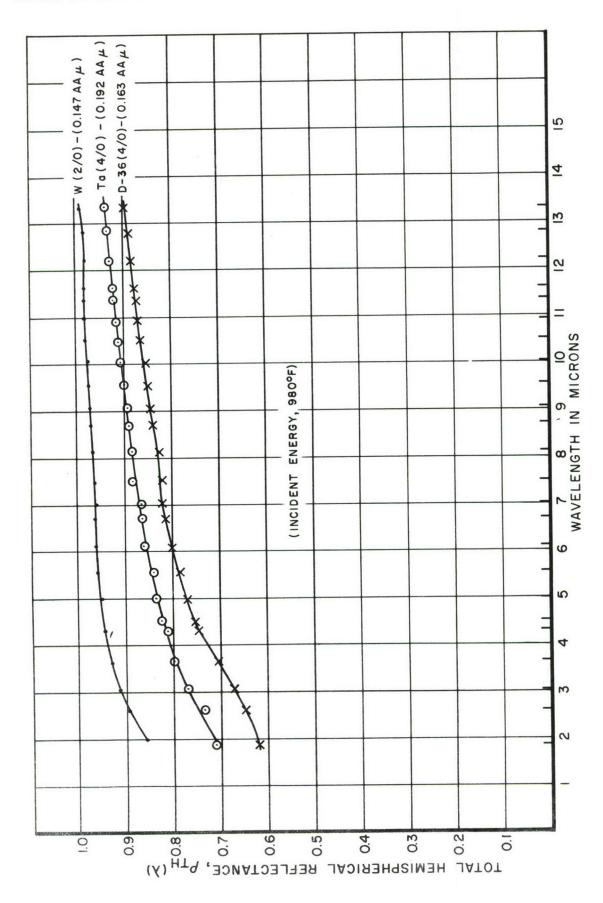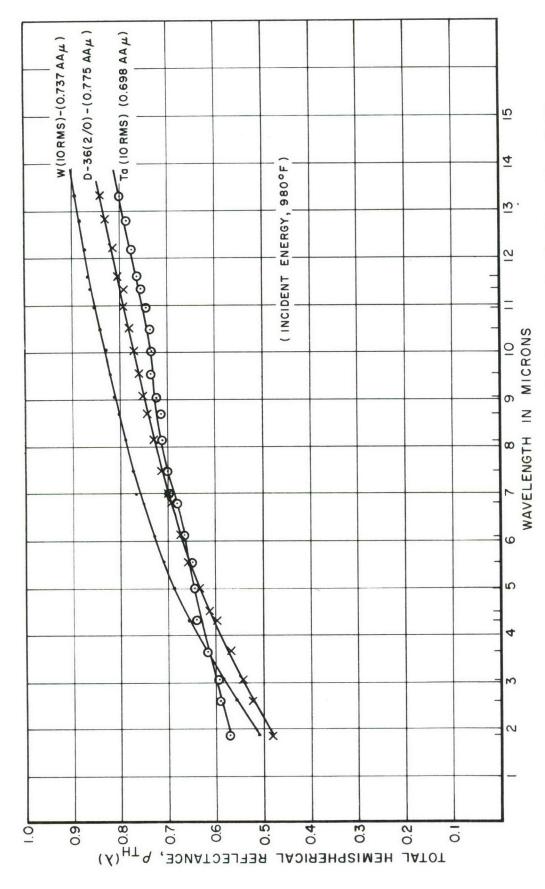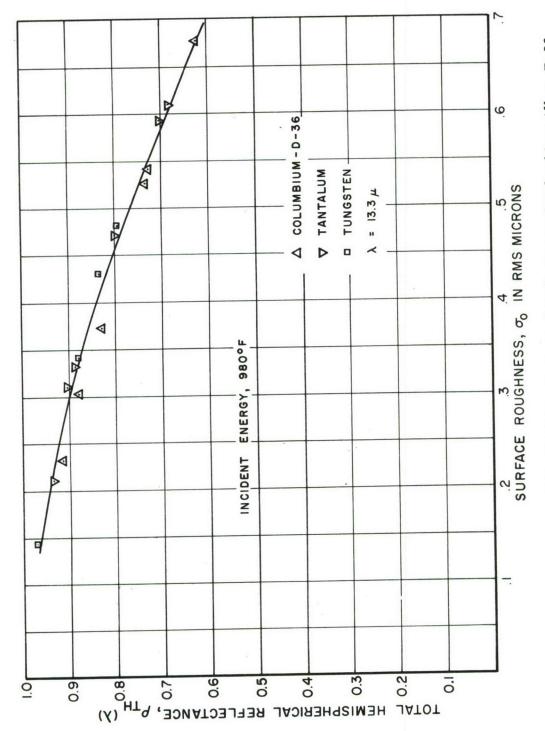
Figure 30. Specular Reflectance of Tungsten as a Function of Wavelength

Figure 31. Comparison of the Total Hemispherical Reflectance of Columbium Alloy, D-36, Tantalum and Tungsten

Figure 32. Comparison of the Total Hemispherical Reflectance of Columbium Alloy, D-36, Tantalum and Tungsten

Figure 33. Comparison of the Total Hemispherical Reflectance of Columbium Alloy, D-36, Tantalum and Tungsten as a Function of the Optical Surface Roughness

SECTION V

DISCUSSION

As indicated earlier, thermal radiation is the only means of transferring heat to or from a system in a space environment. In addition the temperature of the system is directly dependent on the thermal radiation properties, reflectance, emittance and absorption, which, in turn, are dependent on wavelength, material, surface effects, etc. For this report we studied the surface roughness effects on the reflectance of tungsten, tantalum and columbium alloy, D-36.

1. REFLECTANCE AND EMITTANCE

If we consider a system in thermal equilibrium with its environment, be it a space or reentry environment, the thermal radiative properties of reflectance, absorptance and transmittance (for nonopaque materials) are interrelated by reason of the conservation of energy. Thus the total incident energy striking the surface of the system is

$$I = R + A + T \qquad (1)$$

where

> I = incident energy
> R = reflected energy
> A = absorbed energy
> T = transmitted energy

To measure these quantities we must provide a reference for our measurements which is accomplished by using the incident radiation as the reference. Thus we divide each term by the incident energy giving

$$1 = \rho + \alpha + \tau \qquad (2)$$

where

> ρ = the fraction of energy reflected--reflectance
> α = the fraction of energy absorbed--absorptance
> τ = the fraction of energy transmitted--transmittance

Since metals are opaque, due to their extremely high extinction coefficients, the transmittance is zero. Thus

$$1 = \rho + \alpha \qquad (3)$$

Equations 1, 2, and 3 also describe the case for monochromatic energy of wavelength, λ, incident to the surface. Equation 3 would be

$$1 = \rho_\lambda + \alpha_\lambda \qquad (4)$$

Thus, knowing the reflectance of a metal one can determine the absorption and/or emittance of the material.

Emittance, ϵ, is defined as the ratio of the energy radiated per unit area by the surface, W (T), to that radiated per unit area by an ideal or blackbody radiator, $W_B(T)$, at the same temperature. Thus

$$\epsilon = \frac{W(T)}{W_B(T)} \qquad (5)$$

By Kirchhoff's Law the emittance and absorptance are related under equilibrium temperature conditions. Thus

$$\epsilon = \alpha \qquad (6)$$

This law is also valid for monochromatic radiation. Therefore

$$\epsilon_\lambda = \alpha_\lambda \qquad (7)$$

Substituting equation 7 into equation 4 and rearranging terms gives

$$\epsilon_\lambda = 1 - \rho_\lambda \qquad (8)$$

To obtain a better appreciation of the magnitude of the influence of reflectance or emittance on the temperature of a surface, the temperature at a particular emittance has been plotted as a function of the temperature when the emittance of the surface was equal

to unity. (See Figure 34.) As an example, suppose a surface initially had an emittance of 1.0 at 2000°F; the surface temperature would be 2000°F. However, if the emittance changed for some reason to a value of 0.5, the surface temperature would increase to 2500°F. The degree of temperature change increases as higher temperatures are encountered due to the divergence of the curves.

The effect illustrated in this example can be viewed in a different manner. Suppose a material is to be tested at an operating temperature of 4000°F and this temperature is to be measured optically with a pyrometer. A necessary assumption would be the magnitude of the emittance of the material. Suppose further that the emittance of the test specimen was assumed to be 0.6, but in reality it was 0.8; the actual temperature at which the testing would be performed would be 350°F above the 4000°F testing condition.

Thus, as can be seen from the examples, the accurate determination of emittance and/ or reflectance is of paramount importance when it is realized that the temperature of a system's surface can be several hundreds of degrees above the assumed or designed temperature excursion. This may lead to complete system failure. This point can be illustrated further by considering an analysis of Figure 35 (Reference 27). This figure illustrates the steady-state temperature for a re-radiating surface as a function of the surface emittance for different incident heat fluxes. The figure indicates that if the surface emittance could be increased, the surface temperature would decrease.

Using tantalum as an example, the figure indicates that according to the literature, with an emittance of approximately 0.4 a tantalum surface could survive an incident heat flux of approximately 70 Btu/ft^{2}sec and still be useful. However, by integrating the data in Figure 23 and using Equation 8, it is found that the emittance can range from approximately 0.3 for a 0.192 AA μ surface to 0.6 for a 3.0AA μ surface. Using this information, Figure 35 indicates that a tantalum surface could survive an incident heat flux of only 50 Btu/ft^{2}sec with an emittance of 0.3 or would be useful exposed to an incident heat flux of approximately 110 Btu/ft^{2}sec with an emittance of 0.6.

If on a laboratory specimen a design engineer determined the emittance to be 0.6, but in the fabrication of the system using the material a smoother surface finish was obtained, the system would fail at an incident heat flux much lower than anticipated. The same situation exists for tungsten, columbium and other nonopaque materials where the surface greatly influences the optical properties.

The melting points of the refractory metals and alloys are sufficiently high to be used in present and future systems, but their strength properties show a rapid decrease with increasing temperature. However, most important, insofar as reentry applications are concerned, is the fact that the refractory metals cannot withstand elevated temperatures in an oxidizing atmosphere. It is therefore essential to protect these metals with coatings. Coating the refractory metal complicates the correlation of the optical properties data, due to the added influences of mixed oxide emission, volume emission, surface and subsurface chemistry effects, scattering and temperature gradients. It was felt that considerable progress could be made toward correlation by studying a fairly simple system where most of the above complications have been eliminated. The simple system would be the pure refractory metal having no coating or a very thin oxide layer since naturally occurring oxide films have negligible effects at wavelengths longer than 2 μ .

The data generated in this study can be very useful in predicting the emittance of a refractory metal-coating system at temperatures above which the coating becomes transparent and the reflection or emission is from the refractory metal substrate. If the substrate is rough, the emittance will be high; if the substrate is smooth the emittance will be low. Thus with a knowledge of the temperature at which the coating becomes transparent and the surface roughness of the substrate, one can predict the emittance of the system and therefore the temperature of the system's surface.

Further by having a knowledge of the magnitude of the surface roughness or geometric

effect in relation to a simple system, it may be possible to make correlations with more complex systems where the chemistry and geometry of the surface are variable. Knowledge of the magnitude of surface roughness effects will determine whether its effect on the optical properties of a complex system predominate or are masked by the chemistry effects of the surface.

2. SURFACE ROUGHNESS

The dearth of reflectance and emittance data, the lack of surface characterization and the effect of the surface condition on the thermal optical properties are an important, and probably the most often overlooked, parameters in current studies. Therefore, much of the available reflectance and emittance data is of little practical or theoretical value.

To provide a proper interpretation of reflectance and/or emittance data, an accurate characterization of the surface and an understanding of the relationship between the radiative properties and surface roughness must be provided through analytical expressions which relate reflectance and/or emittance as a function of temperature and wavelength to the roughness of opaque materials.

A study of the literature indicates that the basic theories of thermal optical properties deal with the interactions between a quantized electromagnetic field and the electrons and phonons of the material. The reflection, emission, absorption, and transmission of the incident energy by a material can be related to phonon and electron characteristics. Differences in these characteristics point out the basic differences between classes of materials such as metals, dielectrics, and semiconductors.

As indicated above, metals exhibit true optical opacity at all wavelengths. Opacity also implies that emission, absorption and reflection characteristics represent surface phenomena (i.e., the penetration depth of the electromagnetic wave is on the order of 1000$\overset{o}{A}$ at the peak of the incident spectral distribution) and thus the surface characteristics have demonstrated a controlling influence on the optical properties.

Depending upon the wavelength of the incident energy and the degree of surface roughness two approaches have been used to describe the reflectance and emittance from rough surfaces. If the RMS roughness σ_m is much less than the wavelength (λ) of the incident energy (i.e., slightly rough surfaces, $\sigma_m \ll \lambda$), it is necessary to consider the diffraction effects of the surface. Interactions are considered to be in the physical optics region for this situation. For rough surfaces ($\sigma_m \gg \lambda$) it is necessary to consider the interactions in a manner similar to "V" groove analysis (Reference 28) in which gross surface properties influence the average behavior. These interactions are considered to be in the geometrical optics region. This is the region where the effects can be handled in terms of "shape factors," focal lengths, etc. The rough surfaces found in practice may have both diffuse and specular walls in the same "V" groove. They may also have positive and negative slopes along the groove walls. These conditions add to the complications and nullify the ideal assumption of the perfectly diffuse or specular walls and gray surfaces (constant spectral emissivity) used in analyzing the equivalent "V" grooved surfaces.

For this study we have considered only the diffraction effects of the surface for surface roughness values less than 40 RMS microinches or 1.0 AAμ. For these cases the minimum value of the ratio of the roughness to the wavelength is much less than one ($\sigma_{m_1}/\lambda_1 = 0.00447$) and the maximum value is also much less than one ($\sigma_{m_2}/\lambda_2 = 0.08712$).

Figure 36 illustrates a portion of typical surface roughness profile trace made by the movement of a fine pointed stylus over a typical surface. The trace is typical of a true surface profile to the extent that accuracy of representation depends on the fineness of the stylus or resolution of the instrument and the hardness of the material. If the point of the stylus is too large, it will not touch the bottom of the valleys. If the material is too soft the stylus will roundoff the peaks, thus scratching the surface.

The parameters used to characterize a typical surface are also illustrated in this figure. To obtain these parameters it is necessary to establish a line parallel to the

direction of motion of the stylus which acts as a reference line from which profile parameters can be measured. This line is called the center or mean line and is represented by the x-axis in Figure 36.

The RMS roughness can be calculated from this figure by considering the mean-squared deviations of the profile from the center line. Thus

$$\sigma_m = \left[\frac{1}{n} \sum_{i=1}^{i=n} y_i^2 \right]^{\frac{1}{2}} \qquad (9)$$

where n = the total number of vertical measurements.

Another parameter often quoted as surface roughness is the Arithmetic Average (AA). Thus

$$AA = \frac{1}{n} \sum_{i=1}^{i=n} |y_i| \qquad (10)$$

The RMS roughness measurement gives greater weight to the larger peaks causing this measurement to be approximately 11 percent higher than the AA rooughness measurement.

The average peak-to-valley height $(y_1 - y_2)$ is the sum of the average peak heights and the valley depths measured from the center line. The average peak-to-peak distance $(x_2 - x_1)$ decreases in importance as the randomness of the profile increases due to the arbitrary judgment in distinguishing primary peaks at x_1 and x_2 and secondary peaks such as the one at x_3 (Reference 23).

The average profile slope is computed by dividing the average peak-to-valley height by half the average peak-to-peak distance. Thus

$$\frac{dy}{dx} = \frac{1}{2} \frac{(y_1 - y_2)}{(x_2 - x_1)} \qquad (11)$$

Using the above σ/λ values and the assumptions of Bennett and Porteus (Reference 11) we assumed that the curves of the total hemispherical reflectance vs surface roughness

would be similar to those obtained by Birkebak, et al. (Reference 22). The reflectance was a smooth function of the surface roughness having no discontinuities and beyond about a 1.0 μ surface finish the hemispherical reflectance was independent of further increases in the surface roughness. However, as indicated in Figures 22, 26 and 27 we did find discontinuities and a slight decrease in reflectance for large surface roughness values. These effects have been attributed to secondary effects. The discontinuity has been attributed to differences in the surface stress or differences in the surface energy caused by the surface preparation technique. The decrease in the reflectance for very rough surfaces (3.0 AA μ peak-to-valley) is attributed to shadowing, multiple reflections, and specular reflections from smooth peak-to-valley slopes.

Other attempts were made to describe the surface using optical techniques (see Figure 28) since Bennett and Porteus (Reference 11) derived expressions relating the surface roughness of a plane surface to its specular reflectance at normal incidence. The assumption was made in the derivation that if light of a sufficiently long wavelength is used for reflectance measurements, the measured specular reflectance is a function only of the RMS height of the surface irregularities. However, for very rough surfaces found in practice (peak-to-valley heights approximately 1.0 AA μ or larger) the effects of shadowing and multiple reflections become increasingly important at very short wavelengths which tends to invalidate the derivation. In addition the derivation does not consider the effect of surface stress or differences in surface energy due to differences in surface preparation. The magnitudes and relations of these parameters to the surface reflectance and/or emittance become nebulous. The criteria of $\sigma/\lambda \ll 1$ has little meaning. In this work the values ranged from 0.0045 to 0.0871 and no significant correlation could be obtained between the reflectance and surface roughness for the samples of the same material having different degrees of surface roughness. Even Bennett and Porteus (Reference 11) point out that the derivation of the relationship between reflectance and surface roughness is not valid when $\sigma/\lambda \ll 1$, and from the literature there appears to be no more definite limits set on this ratio.

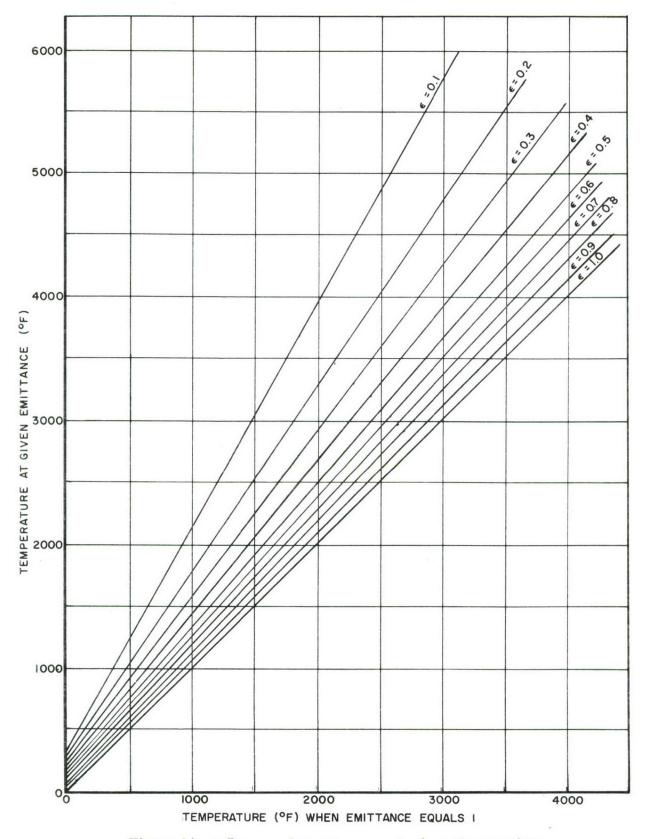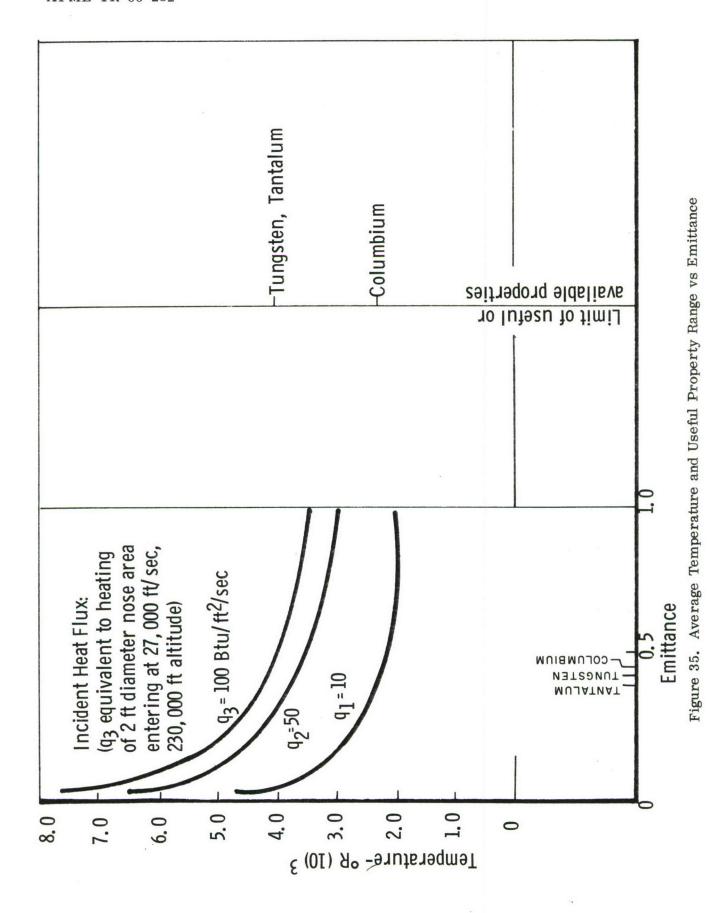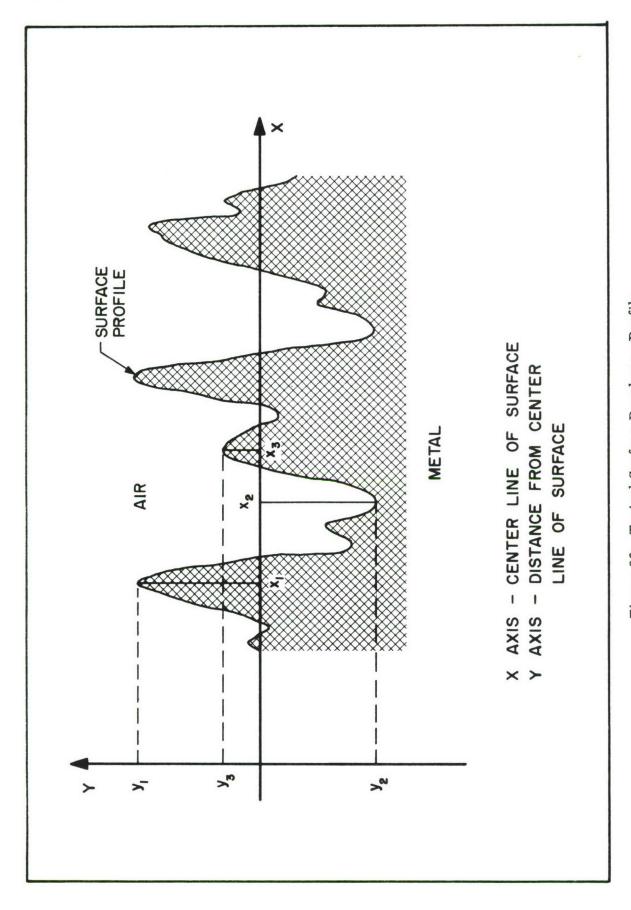Figure 34. Influence of Emittance on Surface Temperature

Figure 35. Average Temperature and Useful Property Range vs Emittance

X AXIS — CENTER LINE OF SURFACE
Y AXIS — DISTANCE FROM CENTER
LINE OF SURFACE

Figure 36. Typical Surface Roughness Profile

SECTION VI

CONCLUSIONS

It can be seen that by neglecting surface roughness, literature values of emittance and reflectance are meaningless. Some indication must be given of the type of surface being studied. An "as-received" surface has no meaning for obvious reasons, and a "polished" surface is about as meaningless unless a description of the polishing technique is given.

The experimental results have indicated that for the columbium alloy, D-36:

(1) Surface roughness variations from 0.163 AAμ to 1.015 AAμ caused the total hemispherical reflectance to change 20 percent at short wavelengths (2.0μ) and 28 percent at longer wavelengths (13.0μ);

(2) Surface roughness variations from 0.6 AAμ to 3.0 AAμ caused the specular reflectance to change 22 percent at the short wavelengths and 75 percent at longer wavelengths;

(3) Discontinuities appear in the total hemispherical reflectance vs surface roughness data at 1.0 AAμ which are attributed to differences in surface energy produced by surface stresses induced by the surface preparation technique.

For pure tantalum the experimental results showed that:

(1) Surface roughness variations from 0.192 AAμ to 3.0 AAμ caused essentially the same magnitude of changes as for columbium alloy, D-36, namely, 26 percent change in total hemispherical reflectance at short wavelengths and 25 percent change at the longer wavelengths;

(2) The same surface roughness variation as above caused the specular reflectance to change 56 percnet at short wavelengths and 75 percent at longer wavelengths;

(3) The "hump" in the total hemispherical reflectance vs surface roughness data

was attributed to differences in the surface stress produced by the surface preparation technique;

(4) Using Center Line Average data to characterize the surface gave rise to a discontinuity in the total hemispherical reflectance vs surface roughness data at approximately 0.32 CLAμ;

(5) Total hemispherical reflectance appears to be a second order function of the optical surface roughness at wavelengths longer than 9.0μ; however, perturbations appear in the data at shorter wavelengths due to inadequacies of the theoretical treatments.

The experimental data for pure tungsten indicated that:

(1) Surface roughness variations from 0.065 AAμ to 2.03 AAμ caused the total hemispherical reflectance to change approximately 38 percent at short wavelengths and 15 percent at longer wavelengths;

(2) The same surface roughness variation caused a spectral reflectance change of approximately 88 percent at short wavelengths and 85 percent change at longer wavelengths.

For all three metals a surface roughness from 0.7 to 0.8 AAμ appeared to be a transition type surface (changing from diffuse to specular as a function of wavelength) over the 2 to 13 wavelength range.

Changes in the total hemispherical reflectance of columbium alloy, D-36, tantalum and tungsten due to the elemental make-up of the sample are approximately 16 percent. However, changes in the total hemispherical reflectance due to roughening the surface range from 20 to almost 40 percent.

The total hemispherical reflectance at long wavelengths plotted as a function of the optical surface roughness is independent of material

effects, and indicates that a reflectance measurement can give a direct indication of the surface roughness.

Due to the divergence of the curves in Figure 33, an error in the true temperature of a material of several hundreds of degrees depending on the temperature level and the magnitude of the true emittance. Inadequate predictions of the capability of a system to withstand an incident heat flux exist when the surface conditions are not adequately described.

The results of this study indicate that the surface roughness influences the radiative properties of metals. This influence is drastic in some cases, such as the specular reflectance. It is still not possible to quantitatively predict from theoretical treatments the radiative properties over a wide wavelength range of a specifically prepared surface without experimental verification of the surface roughness and the reflectance of the surface. This is due in part to effects of shadowing, multiple reflections, and minute oxide layers at short wavelengths ($\sigma > \lambda$), contamination of the surface, and surface stress at longer wavelengths ($\sigma < \lambda$), All of which have been indicated as second order effects in this study. Further studies are needed to spearate the effects of each of these variables and to determine the magnitude of their influence. As engineers become concerned with these effects and report data accordingly, improvements in the accuracy of the data will be forthcoming. This is a necessary prerequisite to the control and prediction of radiative properties.

REFERENCES

1. J.A. Coffman, et al., <u>Carbonization of Plastics and Refractory Materials Research</u>, <u>WADD-TR-60-646. Pt II</u>, Wright Air Development Division, Wright-Patterson Air Force Base, Ohio, January 1963.

2. L.A. Jones, "Colorimetry: Preliminary Draft of a Report on Nomenclature and Definitions," J. Opt. Soc. Am., Vol 27, No. 6. June 1937, pp. 207-213.

3. A.G. Worthing, "Temperature Radiation Emissivities and Emittances," <u>Temperature, Its Measurement and Control in Science and Industry</u>, Reinhold Publishing Corp., New York, New York, 1941. p. 1164.

4. W.H. Harrison, et al., <u>Standardization of Thermal Emittance Measurements, WADC TR-59-510, Pt. IV</u>, Wright Air Development Center, Wright-Patterson Air Force Base, November 1963.

5. Lord Rayleigh, "Polish," Nature. Vol 64. No. 1659. August 1901, pp. 385-388.

6. W.W. Coblenz, <u>NBS</u>, Vol 9. National Bureau of Standards, Washington, D.C., 1913, p. 283.

7. A.F. Gorton, Phys. Rev., Second Series, Vol 7, 1916, pp. 66-78.

8. T.K. Chinmayandam, "On the Specular Reflection From Rough Surfaces," Phys. Rev., Vol 13. 1919, p. 96.

9. P. Beckmann and A. Spizzichino, <u>The Scattering of Electromagnetic Waves From a Rough Surface</u>. Macmillan Co., New York, 1963.

10. H. Davies, "The Reflection of Electromagnetic Waves From a Rough Surface," <u>Proceedings, Inst. Elec. Eng.</u>, Vol 101, 1954, p. 209.

11. H.E. Bennett and J.O. Porteus, "Relation Between Surface Roughness and Specular Reflectance at Normal Incidence," J. Opt. Soc. Am., Vol 51, No. 2, February 1961, pp. 123-129.

12. V. Twersky, "On the Nonspecular Reflection of Electromagnetic Waves," J. Appl. Phys., Vol 22, No. 6. June 1951, pp. 825-835.

13. H.E. Bennett, <u>Symposium on Thermal Radiation of Solids</u>, National Aeronautics and Space Administration, Washington, D.C., 1965, p. 145.

14. R.A. Seban and R.E. Rolling, <u>Thermal Radiation Properties of Materials</u>, <u>WADD-TR-60-370. Pt II</u> Wright Air Development Division, Wright-Patterson Air Force Base, Ohio, March 1962.

15. E. Hagen and H. Ruben, <u>Ann. d. Physik</u> Vol 11, No. 4, 1903, p. 873.

16. D.A. Russell, "Spectral Reflectance of Rough Surfaces in the Infrared, "M.S. Thesis, 1961, University of California at Berkeley.

17. P. Drude, <u>Ann. d. Physik</u>, Vol 64, 1898, p. 159.

REFERENCES (Cont'd)

18. S. Roberts, "Optical Properties of Nickel and Tungsten and Their Interpretation According to Drude's Formula," Phys. Rev., Vol 114, No. 1, April 1959, pp. 104-115.

19. T. Holstein, Westinghouse Res. Labs. Repts. 60-94698-3, R1, R2, R3, M8.

20. D.P. DeWitt, Symposium on Thermal Radiation of Solids, National Aeronautics and Space Administration, Washington, D.C., 1965. p. 141.

21. R.E. Gaumer, Ibid., p. 135.

22. R.C. Birkebak, et al., "Effect of Surface Roughness on the Total Hemispherical and Specular Reflectance of Metallic Surfaces," A.S.M.E. Jour on Heat Transfer, Vol 86, Series C, No. 2, May 1964, pp. 193-199.

23. R.E. Rolling, et al., Investigation of the Effect of Surface Condition on the Radiant Properties of Metals, AFML-TR-64-363, Air Force Materials Laboratory, Wright-Patterson Air Force Base, Ohio, November 1964.

24. R.H. Keith, "The Preparation of Samples For Determination of Their Infrared Optical Properties Using the Perkin-Elmer 13/205 Apparatus," UDRI-TR-64-105. The University of Dayton Research Institute, Dayton, Ohio, August 1964.

25. N. Ashby and K. Schocken, Symposium on Thermal Radiation of Solids, National Aeronautics and Space Administration, Washington, D.C. 1965, p. 63.

26. The Bendix Corporation. "Surface Texture, Surface Measurement and the American Standard ASA B46.1-1962," Micrometrical Division Technical Bulletin.

27. Dally, J.W., Design Data For Materials Employed in Thermal Protected Systems on Advanced Aerospace Vehicles, ML-TDR-64-204, Vol III, Air Force Materials Laboratory, Wright-Patterson Air Force Base, Ohio, August 1965.

28. J. Psarauthakis, "Apparent Thermal Emissivity From Surfaces With V-Shaped Grooves," AIAA Journal, Vol 1, No. 8. 1963, p. 1879.

APPENDIX I

EMITTANCE FURNACE AND SPECTROPHOTOMETER CALIBRATION

APPENDIX I

EMITTANCE FURNACE AND SPECTROPHOTOMETER CALIBRATION

1. EMITTANCE FURNACE CALIBRATION

Figure 37 shows the optical path of the Perkin-Elmer model 205 attachment for measuring emittance. A comparison of this figure and Figure 4 shows that the only differences between the emittance and reflectance modes of operation are: (1) for the emittance mode the specimen is heated by a separate furnace and, (2) a final mirror, M24, has been removed from the optical path. The specimen is placed over the top of a vertical heated cavity referred to as the emission sample holder. The radiant flux is conducted to the front face. There the energy is emitted to the optical system and is characteristic of the material.

The surface temperature of the specimen is maintained at the same temperature as the hohlraum reference cavity. The heated specimen is the source for the spectrophotometer sample beam while an area on the hohlraum cavity wall continues to serve as the blackbody reference source. By establishing and maintaining the same set point temperature for both the specimen and the cavity wall, an absolute measurement of the specimen's normal emittance at the set point temperature is obtained and recorded by the spectrophotometer.

The temperature of the emittance sample holder or emittance furnace is controlled by a similar L and N electromax signal controller as discussed in the section "Description of Equipment." The temperature control signal is derived from a single thermocouple which monitors the "back-face" temperature of a specimen in the furnace. This is a disadvantage in some respects if the sample is a poor conductor or is fairly thick. Either of these conditions can cause a temperature difference to exist between the emitting front surface and the back surface and therefore produces a temperature difference between the specimen and the reference which must be accounted for if accurate emittance determinations are to be made.

To calibrate this temperature controller a 36-gage chromel-alumel thermocouple was attached to the front surface of a specimen. A hole was drilled into the specimen and a hollow alumina tube placed through the hole. Another 36-gage chromel-alumel thermocouple was placed through the hollow tube and positioned at the mid point of the emission sample holder cavity.

The diagram in the lower right portion of Figure 38 represents a cross section through this emittance furnace. The thermocouple T_1 measures the cavity temperature; T_2 is the back face temperature which is sensed by the L and N temperature controller, and is referred to as "dial temperature." T_3 is the front face temperature at which the hohlraum reference is set and maintained.

Figure 38 is a plot of the temperature dial reading on the L and N controller versus the temperature of the front face and the probe as measured by a calibrated potentiometer. Since the controller is an "on-off" type controller, a maximum and a minimum temperature results. As can be seen in this figure the two curves diverge. At a given control temperature the front face temperature is much lower than the cavity interior temperature due to the emittance of the specimen. The energy emitted to the cooler surroundings reduces the temperature of the surface. The curves diverge because the temperature difference between the surroundings and the cavity is increasing along with an increase in emittance as the temperature increases.

2. SPECTROPHOTOMETER EMITTANCE MODE CALIBRATION

Oxidized inconel, oxidized kanthal, and polished platinum were furnished by the National Bureau of Standards (NBS) for high, medium, and low emittance standards respectively. Each of these standards was measured with our equipment and the data compared with that generated by NBS (Reference 4). The

results of this comparison are illustrated in Figures 39, 40, and 41. In each case the temperature of the standard was controlled to that of the reference to within 1°C. The temperature in each case was 527°C (980°F). Each data point is an average of 5 measurements.

Figure 39 shows that even with careful temperature adjustments of reference and standard there is still an error ranging from 4 to 12 percent on the short wavelength side of the blackbody peak at 3.5μ where any temperature difference between reference and standard is greatly accentuated. Our data follows the NBS curve except at the extreme ends of the wavelength range. Similar comments can be made concerning Figure 40 for the intermediate emittance standard, oxidized kanthal.

Figure 41 shows that for low emittance specimens our instrument would give values approximately 0.03 emittance units too high except for wavelengths shorter than 2.5μ. See Appendix II for Emittance Correction Factors.
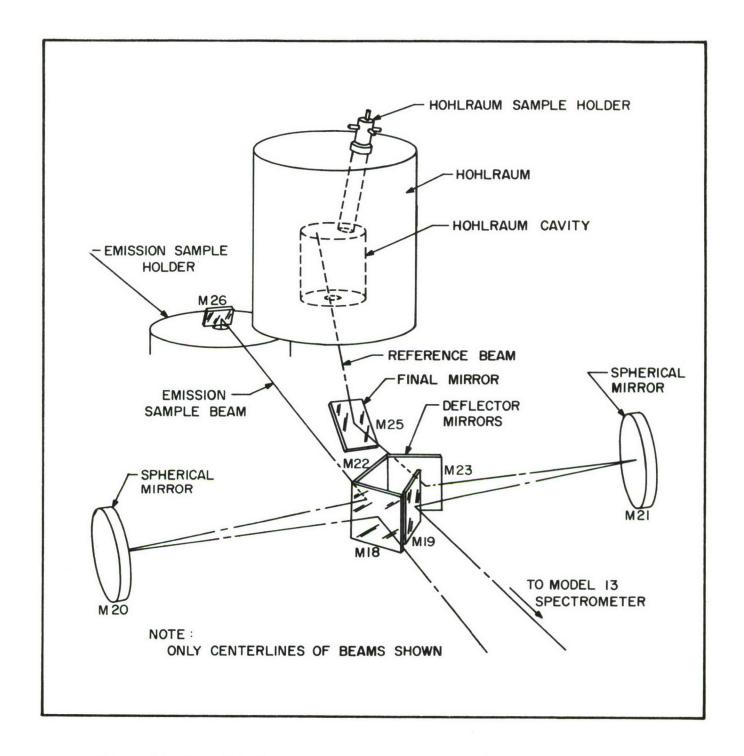
Figure 37. Optical Path to Spectrophotometer for Emittance Measurements
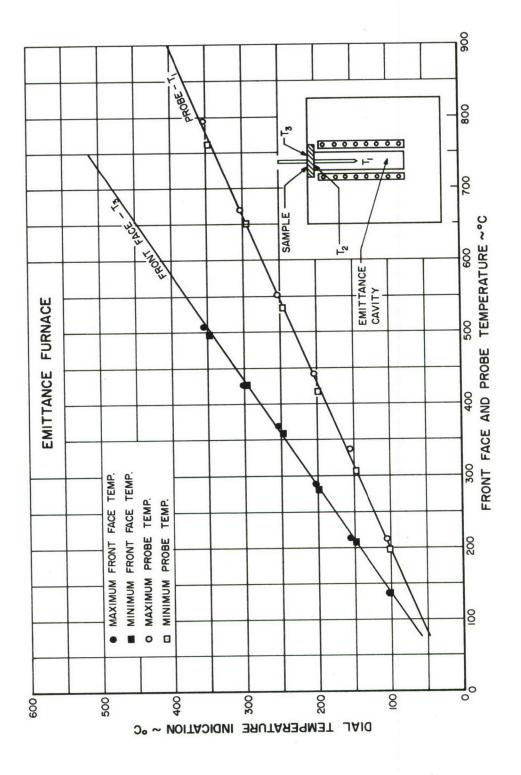
Figure 38. Temperature Calibration for Emittance Furnace
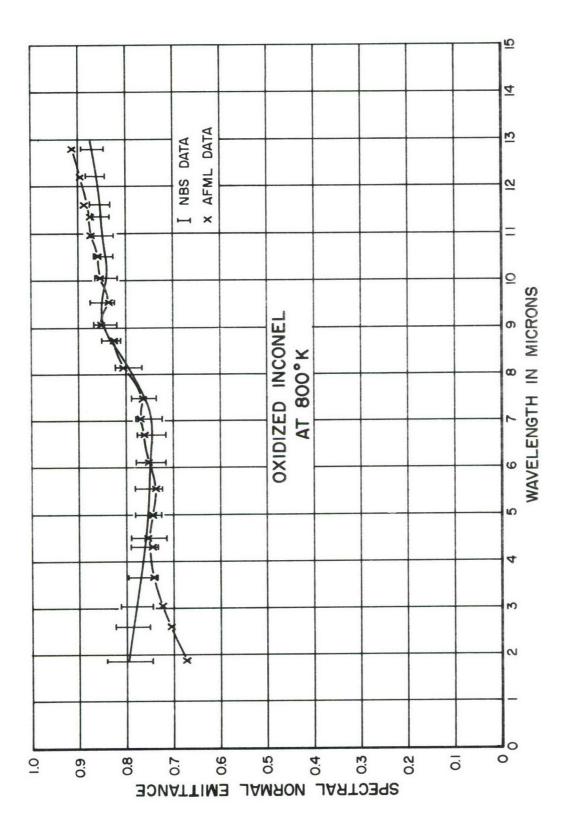
Figure 39. Correlation of AFML Data with NBS Data for Oxidized Inconel at 980° F (800° K)
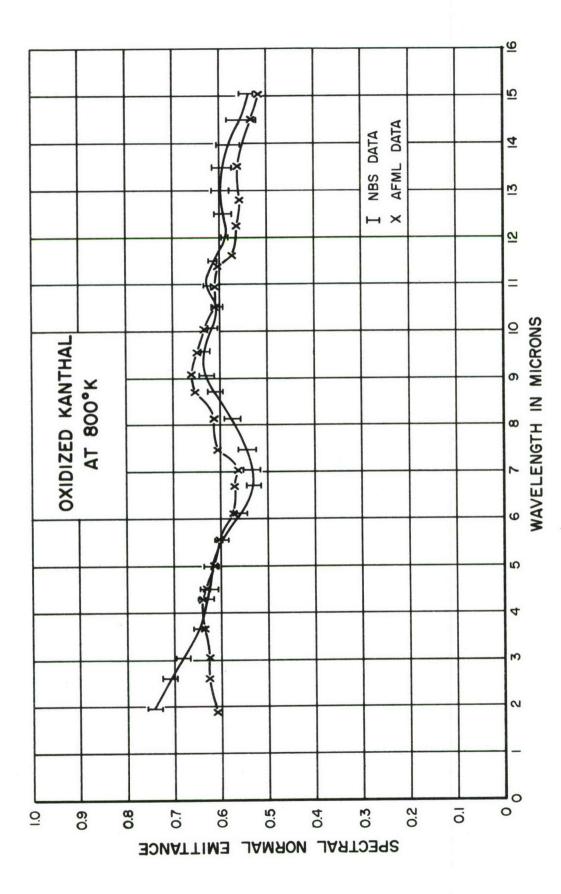
Figure 40. Correlation of AFML Data with NBS Data for Oxidized Kanthal at 980° F (800° K)
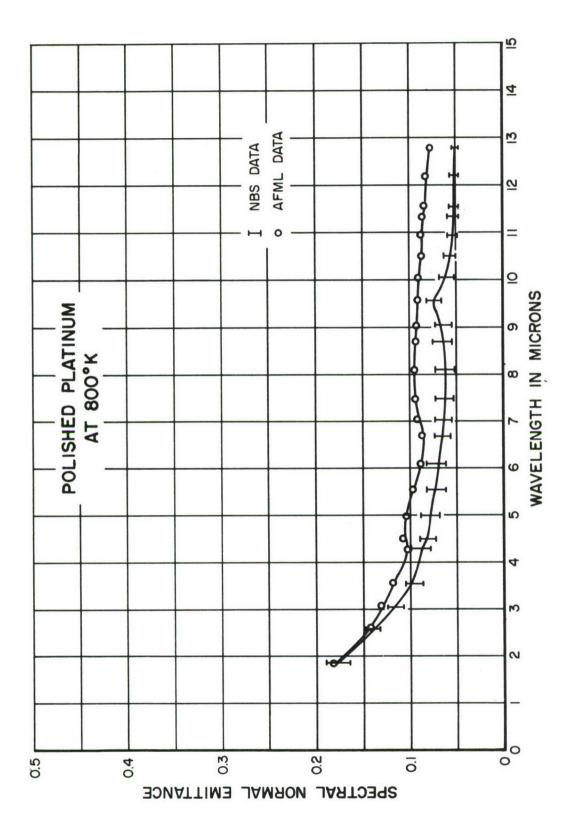
Figure 41. Correlation of AFML Data with NBS Data for Polished Platinum at 980° F (800° K)

APPENDIX II

EMITTANCE CORRECTION FACTORS

APPENDIX II

EMITTANCE CORRECTION FACTORS

Table III shows the correction factor in emittance units to add to specimen emittance values at each wavelength for each emittance range. These values can be used to calculate the magnitude of the error at several wavelength points.

Figure 42 is a plot of the deviation of the emittance data as a function of wavelength for the three standards. All the error in the emittance data generated between 5.8 and 13.0 microns was positive and averaged approximately 0.025 emittance units. For the polished platinum data all corrections were positive from 1.88 to 12.8 μ Below 4.0 μ the corrections are negative for oxidized inconel and kanthal. The oxidized kanthal data shows negative deviations between 4.8 and 5.8 μ .

TABLE III
EMITTANCE CORRECTION FACTOR

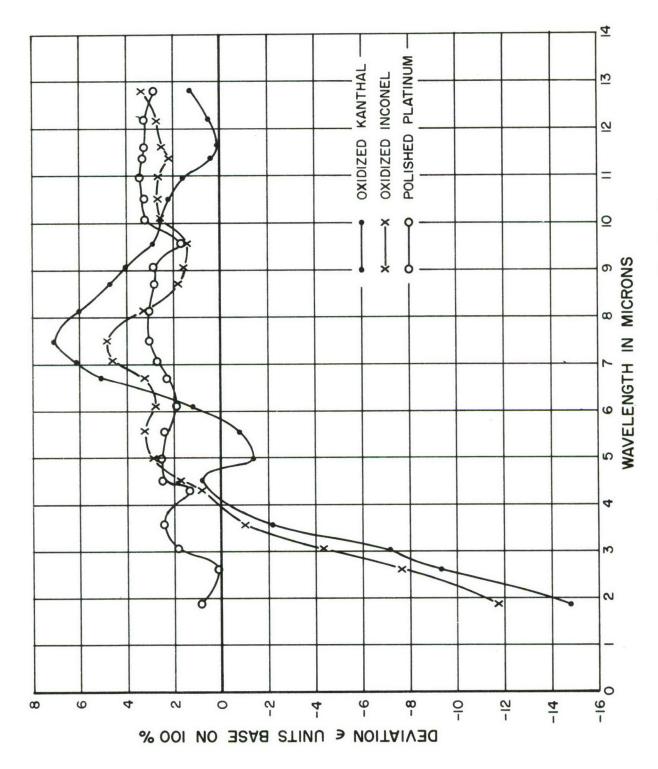| λ	OXIDIZED INCONEL		OXIDIZED KANTHAL		POLISHED PLATINUM	
	ϵ	Correction 1.0 to 0.7	ϵ	Correction 0.7 - 0.4	ϵ	Correction Below 0.4
1.88	79.2	+ 11.8	74.3	+ 14.8	17.7	- 0.8
2.60	78.7	+ 7.7	71.0	+ 9.3	14.0	- 0.1
3.02	77.7	+ 4.4	68.2	+ 7.2	11.5	- 1.8
3.65	76.5	+ 1.0	64.8	+ 2.2	9.5	- 2.4
4.30	76.1	- 0.8	63.1	0.0	8.9	- 1.3
4.50	75.2	- 1.7	62.5	- 0.8	8.1	- 2.5
4.99	75.3	- 2.9	62.2	+ 1.4	7.8	- 2.5
5.54	75.0	- 3.2	59.6	+ 0.8	7.3	- 2.4
6.10	74.8	- 2.8	55.7	- 1.2	6.9	- 1.9
6.70	74.6	- 3.2	53.2	- 5.1	6.4	- 2.3
7.01	75.0	- 4.6	53.4	- 6.1	6.4	- 2.7
7.49	75.9	- 4.8	54.3	- 7.1	6.3	- 3.0
8.12	79.4	- 3.2	57.5	- 6.0	6.2	- 3.1
8.70	83.0	- 1.8	61.2	- 4.7	6.5	- 2.8
9.05	84.3	- 1.6	63.0	- 4.0	6.4	- 2.8
9.55	84.7	- 1.4	63.3	- 2.9	7.4	- 1.6
10.03	83.9	- 2.5	61.8	- 2.6	5.9	- 3.2
10.50	84.4	- 2.6	60.5	- 2.2	5.6	- 3.2
10.94	84.6	- 2.6	62.9	- 1.6	5.4	- 3.4
11.35	85.2	- 2.2	63.2	- 0.4	5.3	- 3.3
11.61	85.5	- 2.5	59.9	- 0.1	5.2	- 3.2
12.21	86.2	- 2.7	58.6	- 0.5	5.1	- 3.2
12.80	86.9	- 3.3	59.9	- 1.3	5.0	- 2.8

Figure 42. Deviation of Emittance Data vs Wavelength

APPENDIX III

CALIBRATION OF SPECTROPHOTOMETER COMPONENT PARTS

APPENDIX III

CALIBRATION OF SPECTROPHOTOMETER COMPONENT PARTS

1. LITTROW MIRROR ANGLE

When a new or different prism is installed in the monochromator for the first time the Littrow mirror (M9 in Figure 4) must be adjusted in order that the "wavelength index" drum values can be accurately related to wavelengths in microns. The angle the Littrow mirror makes with the prism determines the portion of the spectrum which passes through the exit slit, S2, of the monochromator at any given position of the drum. The angle is set for any given prism by rotating mirror M11 out of the optical path. This allows the light from a mercury arc lamp, placed at the external detector position, to traverse the optical path of the monochromator in a reverse manner. Proper alignment is attained by rotating the Littrow mirror until the mercury green line (5460.7Å) passes through the entrance slit, S1. The monochromator is now indexed and the wavelength index drum fixed in relation to the Littrow mirror angle.

2. MONOCHROMATOR

a. Wavelength Calibration

A wavelength calibration was made of the spectrophotometer with the sodium chloride prism mounted in the monochromator. The absorption spectrum of a 0.072 mm thick polystyrene film was recorded using the hohlraum cavity at 980°F as a source. The absorption peaks having known wavelengths were identified, and for each the observed wavelength drum position was plotted as a function of the known wavelength of the peak. All the points fell on a smooth line giving a calibration curve between 2 and 13μ (see Figure 43).

b. Linearity

The input to the recorder of the instrument is a signal which consists of the ratio of radiative fluxes from a reference source and the specimen under observation. Depending on the specimen material, this ratio may vary from near zero to unity. Experimental traces of the zero and 100 percent lines are run, and if the instrument is performing satisfactorily, the response over the calibrated wavelength range will be such that the reference-specimen flux ratios will be recorded with exact linearity. Before conducting optical property calibrations and measurements it is necessary to check the degree of linearity.

Deviations from overall linearity may be caused by optical misalignments, by deviations in the response of the detector and/or detector-amplifier. Overall system performance in this respect is best established by using sector disc attenuators. A sector disc attenuator consists of a variable speed motor with a slotted disc mounted on its shaft. The width of each slot in the disc is such that, with the motor operating at approximately 1300 rpm, the effective transmittance of the disc can be made a certain percentage of the incidence flux. The attenuator is placed in the sample beam of the instrument with the direction of rotation opposite to that of the chopper. The spectrophotometer is operated in the 100 percent mode (reference source in both beams) and the transmittance of the sector disc attenuator measured. The height of the recorded signal above an experimentally obtained zero line should be linear and not deviate by more than 1 percent.

Table IV shows the results of checking the complete system for linearity. Three sector disc attenuators were used to check the linearity. Each disc operating at approximately 1300 rpm had an effective transmittance of approximately 25, 50, and 75 percent. The effective transmittance values were not exact due to maching errors. At the 24 wavelength points selected the linearity deviation was calculated from the average effective transmittance for the 25 percent case, the errors in linearity ranged from +1.6 to -0.6 percent; for 50 percent, +0.97 to -0.59 percent; and for 75 percent, +0.42 to -0.38 percent.

Since nonlinearities arising from optical elements were not felt to be significant

TABLE IV

LINEARITY DEVIATION

λ*	25%	Δ AV	50%	Δ AV	75%	Δ AV
1.88	25.9	0.021 -	51.0	0.004 -	75.1	0.087 -
2.60	25.9	0.021 -	51.0	0.004 -	75.3	0.113 +
3.02	25.9	0.021 -	51.0	0.004 -	75.4	0.213 +
3.65	25.8	0.079 -	51.1	0.096 +	75.2	0.013 +
4.30	25.9	0.021 -	51.0	0.004 -	75.2	0.013 +
4.50	25.9	0.021 -	50.8	0.204 -	75.0	0.187 -
4.99	25.9	0.021 -	50.9	0.104 -	75.1	0.087 -
5.54	26.3	0.421 +	51.1	0.200 +	75.5	0.313 +
6.10	25.8	0.079 -	50.9	0.104 -	75.3	0.113 +
6.70	25.9	0.021 -	50.8	0.204 -	75.0	0.187 -
7.01	25.8	0.079 -	50.9	0.104 -	75.2	0.013 +
7.49	25.8	0.079 -	50.9	0.104 -	75.1	0.087 -
8.12	25.8	0.079 -	50.9	0.104 -	75.0	0.187 -
8.70	25.9	0.021 -	50.8	0.204 -	75.0	0.187 -
9.05	25.7	0.179 -	50.9	0.104 -	75.0	0.187 -
9.55	25.7	0.179 -	50.7	0.304 -	74.9	0.287 -
10.03	25.8	0.079 -	51.0	0.004 -	75.3	0.113 +
10.50	25.8	0.079 -	51.0	0.004 -	75.2	0.013 +
10.94	25.8	0.079 -	51.0	0.004 -	75.1	0.087 -
11.35	25.9	0.021 -	51.2	0.196 +	75.3	0.113 +
11.61	25.9	0.021 -	51.0	0.004 -	75.2	0.013 +
12.21	25.8	0.079 -	51.2	0.196 +	75.3	0.113 +
12.80	26.0	0.121 +	51.5	0.496 +	75.4	0.213 +
13.30	26.2	0.442 +	51.5	0.496 +	75.4	0.213 +
AV	25.879		51.004		75.187	

ERROR IN LINEARITY:		
+ 1.6%	+ 0.97%	+ 0.42%
- 0.6%	- 0.59%	- 0.38%

*λ - WAVELENGTH IN MICRONS

in our instrument, the slit movement, detector and amplifier components were tested separately for linearity deviations. This is an important step in the calibration procedure since nonlinearities in the detector and the amplifier may tend to cancel and thus would not be discovered in overall linearity checks such as with the sector disc attenuator.

The monochromator is constructed such that the width of the entrance and exit slits are identical and are opened and closed simultaneously. The radiant flux reaching the detector from the monochromator varies as the square of the slit width. A plot of the slit width versus the square root of the chart deflection, therefore, gives the linearity of the detector response. With the spectrophotometer operating in the single-beam, direct mode, the linearity of the thermocouple detector response was measured for several wavelengths throughout the sensitive range of the thermocouple detector. The Perkin-Elmer instruction manual recommends that the linearity be determined at a gain setting of 10. At the midwavelength range ($\sim 6 \mu$) the gain was increased to accenuate any nonlinearities in the amplifing system at this wavelength. The linearity of the detector and amplifier is depicted in Figure 44. Linearity of the amplifier is shown in this figure by the fact that at different amplifier gains and wavelengths the points fall on a straight line. A scatter plate is introduced into the optical system at 11.8μ to reduce scattered light. The introduction of this optical element into the system produced no deviations in linearity. All the points fell on straight lines within 1.6 percent. In the area where the straight line portion of the graph failed to pass through the origin, the failure can be attributed to an error in the slit micrometer dial zero setting and a diffraction effect produced by the extremely narrow slits.

c. Stability

The amplifier system has been designed so that various calibrating signals can be applied across the detector in order to check the stability of the amplifier-recorder network. Thus frequent checks were made of the response and zero drift of the detector. When electronic noise was taken into account, it was found that drift amounts to approximately 2.0 percent over a period of about 1 hour.

3. TEMPERATURE CONTROLLER--RECORDER

The temperature of the reference cavity or hohlraum is controlled by a Leeds and Northrup (L and N) electromax signal controller which is designed to operate as a combined signalling device and a two-position ("on-off") controller. The maximum error for this controller is 0.3 percent or less of the scale span from 0° to 1100°C. The control sensitivity of this controller is a 0.03 mv dead band between "on" and "off." This is roughly equivalent to 1°C with an iron-constantan or chromel-alumel thermocouple.

Due to slight temperature gradients within the cavity, the three thermocouples (see Figure 7 for thermocouple location) read slightly different. This difference is shown in Figure 45. In order to calibrate the controller dial a separate thermocouple was used to probe the cavity (see Figure 45). This temperature is called the true temperature since this would be the average temperature seen by a specimen located within the cavity. The dial temperature indication was plotted as a function of the probe (true) temperature in this figure. The millivolt signals from the probe thermocouple were used to calibrate the hohlraum temperature controller and were measured with a calibrated Rubicon potentiometer.

4. SURFACE ROUGHNESS MEASUREMENTS

Surface roughness measurements were calibrated using a precisely calibrated standard traceable to the National Physical Laboratory, England. The roughness standard is comprised of a series of three grooves of uniform depth (0.38μ) and spacing (50.0μ), etched in a glass plate.

Figure 46 is a trace of the roughness standard. The error in peak-to-valley measurements at this the highest magnification (X6) is only 1.3 percent. At lower magnifications the error is much less. This indicates that the condition of the stylus point is not chipped or worn, or that the instrument is in need of adjustment.
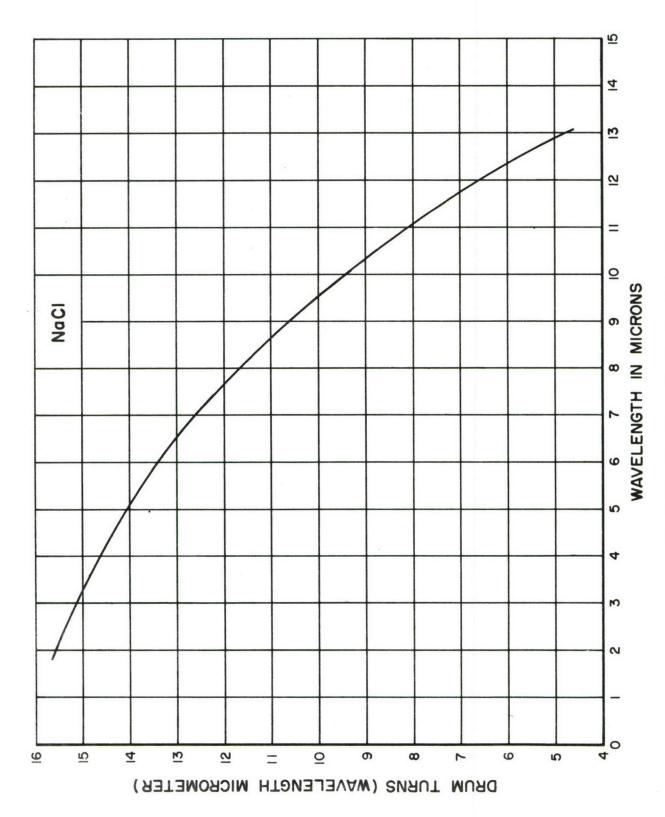
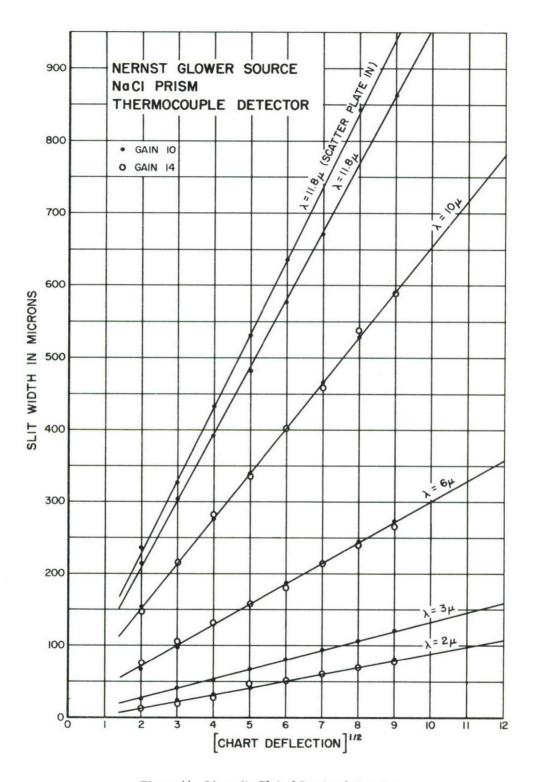Figure 43. Calibration Curve for Spectrophotometer

Figure 44. Linearity Plot of Spectrophotometer
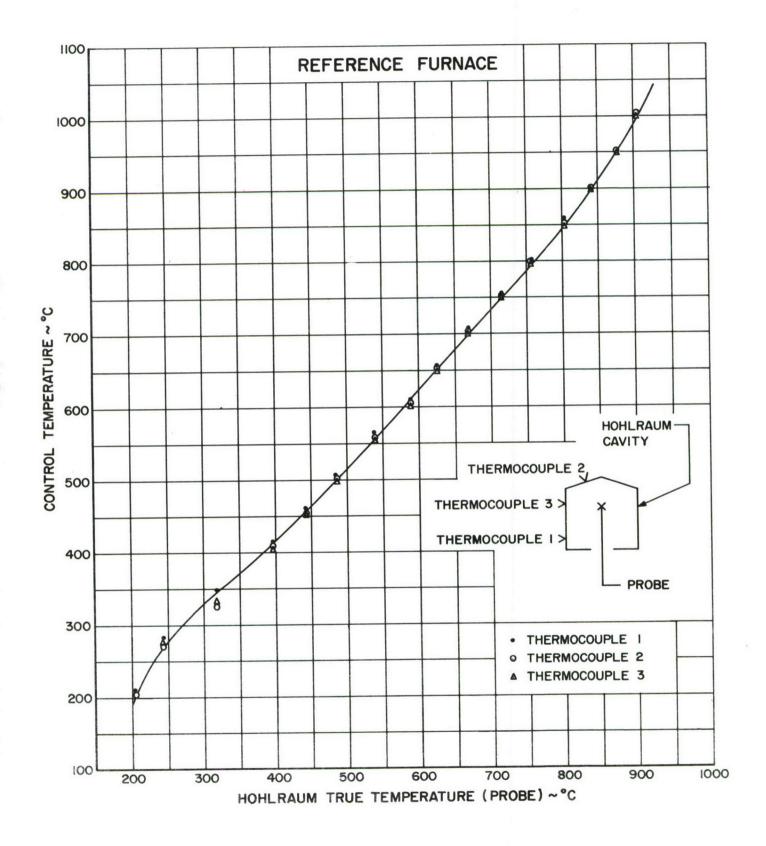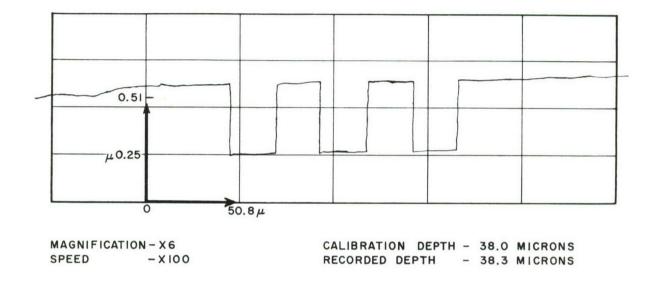
Figure 45. Temperature Calibration for Hohlraum

MAGNIFICATION-X6   CALIBRATION DEPTH – 38.0 MICRONS
SPEED   – X100   RECORDED DEPTH   – 38.3 MICRONS

Figure 46. Profilometer Trace of Roughness Standard

DOCUMENT CONTROL DATA - R&D

(Security classification of title, body of abstract and indexing annotation must be entered when the overall report is classified)

1. ORIGINATING ACTIVITY (Corporate author)	2a. REPORT SECURITY CLASSIFICATION
Air Force Materials Laboratory, Research and Technology Division, Air Force Systems Command, Wright-Patterson Air Force Base, Ohio	2b. GROUP

3. REPORT TITLE

EFFECT OF SURFACE ROUGHNESS ON THE REFLECTANCE OF REFRACTORY METALS

4. DESCRIPTIVE NOTES (Type of report and inclusive dates)

1 May 1965 to 1 May 1966

5. AUTHOR(S) (Last name, first name, initial)

Stevison, Donald F.

6. REPORT DATE	7a. TOTAL NO. OF PAGES	7b. NO. OF REFS
December 1966	94	28

8a. CONTRACT OR GRANT NO.	9a. ORIGINATOR'S REPORT NUMBER(S)
b. PROJECT NO. 7381	AFML-TR-66-232
c. Task No. 738102	9b. OTHER REPORT NO(S) (Any other numbers that may be assigned this report)
d.	

10. AVAILABILITY/LIMITATION NOTICES This document is subject to special export controls and each transmittal to foreign governments or foreign nationals may be made only with prior approval of the Materials Application Division, Air Force Materials Laboratory (MAAE), Wright-Patterson Air Force Base, Ohio 45433.

11. SUPPLEMENTARY NOTES	12. SPONSORING MILITARY ACTIVITY
	Air Force Materials Laboratory, Research and Technology Division, Air Force Systems Command, Wright-Patterson AFB, Ohio

13. ABSTRACT

The influence of surface roughness on the thermal optical properties (reflectance and emittance) of three refractory materials, columbium alloy, D-36, tantalum and tungsten has been studied. Current data obtained by different investigators for the same materials have varied more than 50 percent. Several investigators studying the interaction of radiation with rough surfaces have developed theoretical approaches to correlate thermal optical properties with the material being studied; however, no predictions have been made as to the magnitude of the surface effects. This report establishes several general trends in this direction.

A Perkin-Elmer model 13U Spectrophotometer with a model 205 Reflectance-Emittance attachment was used for all reflectance an emittance measurements. A Taylor-Hobson Talysurf was used to measure the surface roughness of each sample. Two surface roughness preparations were used-random sanding and sandblasting.

As a typical example of the results, the total hemispherical reflectance of tantalum was changed 26 percent at short wavelengths and 25 percent at longer wavelengths by surface roughness values ranging from 0.192 to 3.0 AA microns. The specular reflectance of tantalum changed 56 percent at short wavelengths and 75 percent at long wavelengths for the same range of surface roughness values. Material effects caused a maximum difference of only 16% in the total hemispherical reflectance of these three refractory materials; however, the maximum change in surface roughness caused the total hemispherical reflectance to vary 20 to 40 percent as a function of wavelength.

The influence of second order effects has been observed. The degree to which emittance influences the surface temperature and incident heat flux capabilities of materials is discussed.

DD $_{1\ JAN\ 64}^{FORM}$ **1473**

14. KEY WORDS	LINK A		LINK B		LINK C	
	ROLE	WT	ROLE	WT	ROLE	WT
Surface Roughness						
Reflectance						
Emittance						
Refractory Metals						

INSTRUCTIONS

1. ORIGINATING ACTIVITY: Enter the name and address of the contractor, subcontractor, grantee, Department of Defense activity or other organization *(corporate author)* issuing the report.

2a. REPORT SECURITY CLASSIFICATION: Enter the overall security classification of the report. Indicate whether "Restricted Data" is included. Marking is to be in accordance with appropriate security regulations.

2b. GROUP: Automatic downgrading is specified in DoD Directive 5200.10 and Armed Forces Industrial Manual. Enter the group number. Also, when applicable, show that optional markings have been used for Group 3 and Group 4 as authorized.

3. REPORT TITLE: Enter the complete report title in all capital letters. Titles in all cases should be unclassified. If a meaningful title cannot be selected without classification, show title classification in all capitals in parenthesis immediately following the title.

4. DESCRIPTIVE NOTES: If appropriate, enter the type of report, e.g., interim, progress, summary, annual, or final. Give the inclusive dates when a specific reporting period is covered.

5. AUTHOR(S): Enter the name(s) of author(s) as shown on or in the report. Enter last name, first name, middle initial. If military, show rank and branch of service. The name of the principal author is an absolute minimum requirement.

6. REPORT DATE: Enter the date of the report as day, month, year; or month, year. If more than one date appears on the report, use date of publication.

7a. TOTAL NUMBER OF PAGES: The total page count should follow normal pagination procedures, i.e., enter the number of pages containing information.

7b. NUMBER OF REFERENCES: Enter the total number of references cited in the report.

8a. CONTRACT OR GRANT NUMBER: If appropriate, enter the applicable number of the contract or grant under which the report was written.

8b, 8c, & 8d. PROJECT NUMBER: Enter the appropriate military department identification, such as project number, subproject number, system numbers, task number, etc.

9a. ORIGINATOR'S REPORT NUMBER(S): Enter the official report number by which the document will be identified and controlled by the originating activity. This number must be unique to this report.

9b. OTHER REPORT NUMBER(S): If the report has been assigned any other report numbers *(either by the originator or by the sponsor)*, also enter this number(s).

10. AVAILABILITY/LIMITATION NOTICES: Enter any limitations on further dissemination of the report, other than those imposed by security classification, using standard statements such as:

  (1) "Qualified requesters may obtain copies of this report from DDC."

  (2) "Foreign announcement and dissemination of this report by DDC is not authorized."

  (3) "U. S. Government agencies may obtain copies of this report directly from DDC. Other qualified DDC users shall request through

       _____ ."

  (4) "U. S. military agencies may obtain copies of this report directly from DDC. Other qualified users shall request through

       _____ ."

  (5) "All distribution of this report is controlled. Qualified DDC users shall request through

       _____ ."

If the report has been furnished to the Office of Technical Services, Department of Commerce, for sale to the public, indicate this fact and enter the price, if known.

11. SUPPLEMENTARY NOTES: Use for additional explanatory notes.

12. SPONSORING MILITARY ACTIVITY: Enter the name of the departmental project office or laboratory sponsoring *(paying for)* the research and development. Include address.

13. ABSTRACT: Enter an abstract giving a brief and factual summary of the document indicative of the report, even though it may also appear elsewhere in the body of the technical report. If additional space is required, a continuation sheet shall be attached.

It is highly desirable that the abstract of classified reports be unclassified. Each paragraph of the abstract shall end with an indication of the military security classification of the information in the paragraph, represented as *(TS)*, *(S)*, *(C)*, or *(U)*.

There is no limitation on the length of the abstract. However, the suggested length is from 150 to 225 words.

14. KEY WORDS: Key words are technically meaningful terms or short phrases that characterize a report and may be used as index entries for cataloging the report. Key words must be selected so that no security classification is required. Identifiers, such as equipment model designation, trade name, military project code name, geographic location, may be used as key words but will be followed by an indication of technical context. The assignment of links, rules, and weights is optional.